# Supporting Information

# A Positively Charged Aggregation-induced Emission (AIE) Luminogen, also an Ultra-sensitive Mechanochromic Luminescent Material: Design, Synthesis and Versatile Applications

*Weidong Yin, Zengming Yang, Shaoxiong Zhang, Yuan Yang, Lixia Zhao, Zhao Li, Bo Zhang, Shengjun Zhang, Bingyang Han, Hengchang Ma**

Key Laboratory of Polymer Materials of Gansu Province, Key Laboratory of Eco-Environment-Related Polymer Materials Ministry of Education, College of Chemistry and Chemical Engineering, Northwest Normal University, Lanzhou 730070, P.R. China

E-mail: mahczju@hotmail.com (Ma HC)

# Table of Contents

## 1. General Information

Unless otherwise described, all reagents and solvents were purchased from commercial sources and used without further purification. All the samples were prepared according to the standard methods. For UV and fluorescence spectral data, each data was measured three times and the average value is taken.

## 2. Experimental details

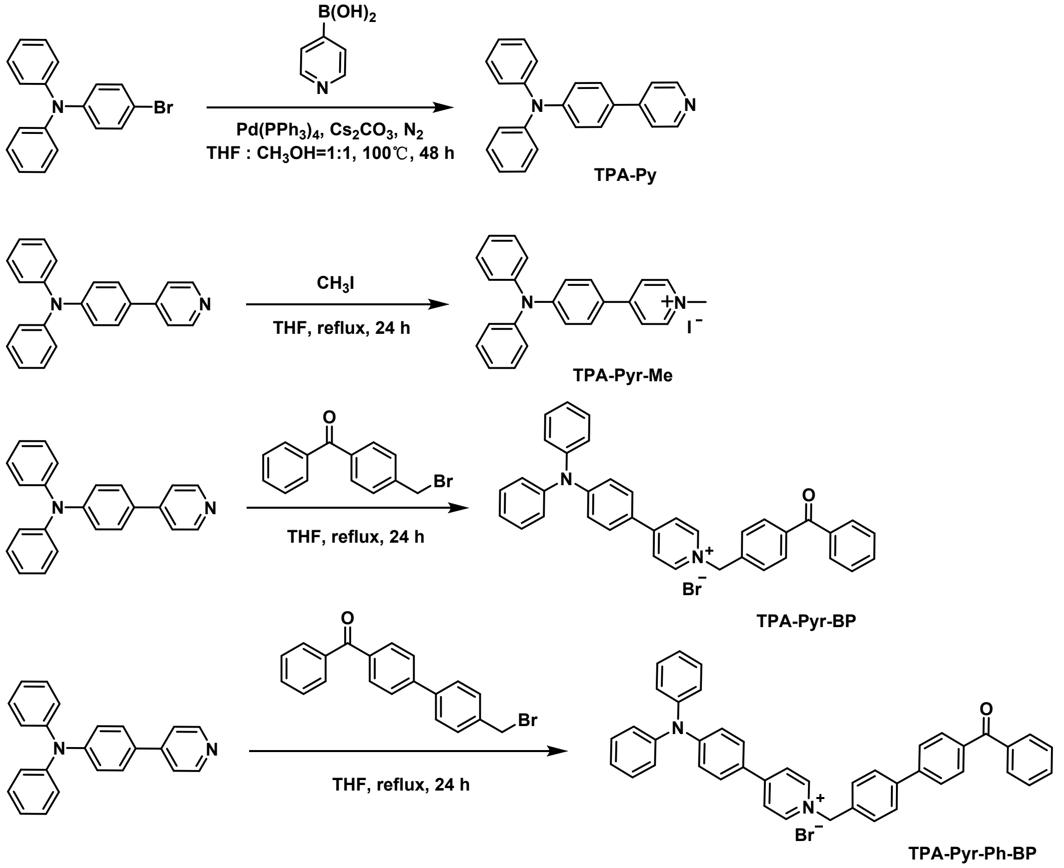


**Scheme S1.** Synthetic routes of TPA-Py, TPA-Pyr-Me, TPA-Pyr-BP and TPA-Pyr-Ph-BP.

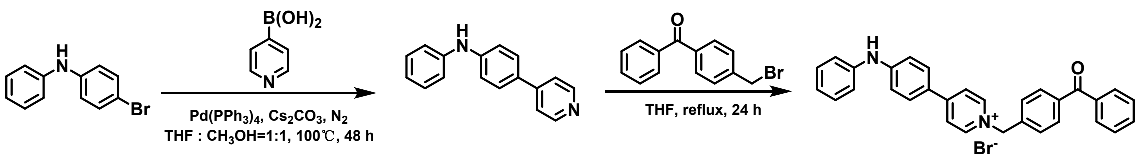


**Scheme S2.** Synthetic routes of DPA-Py and DPA-Pyr-BP.

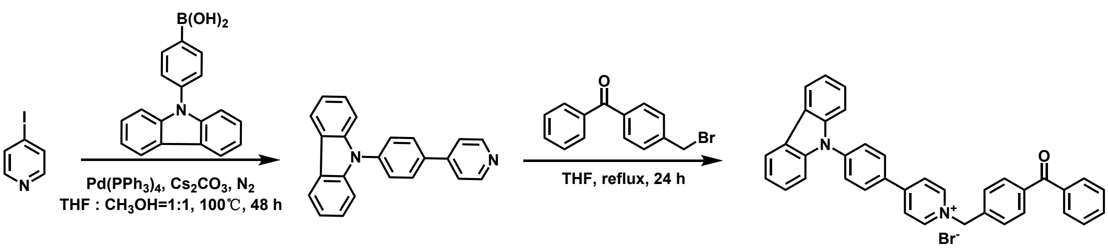

**Scheme S3.** Synthetic routes of CZ-Py and CZ-Pyr-BP.

## 3. [1]H and [13]C NMR Spectra of Compounds.

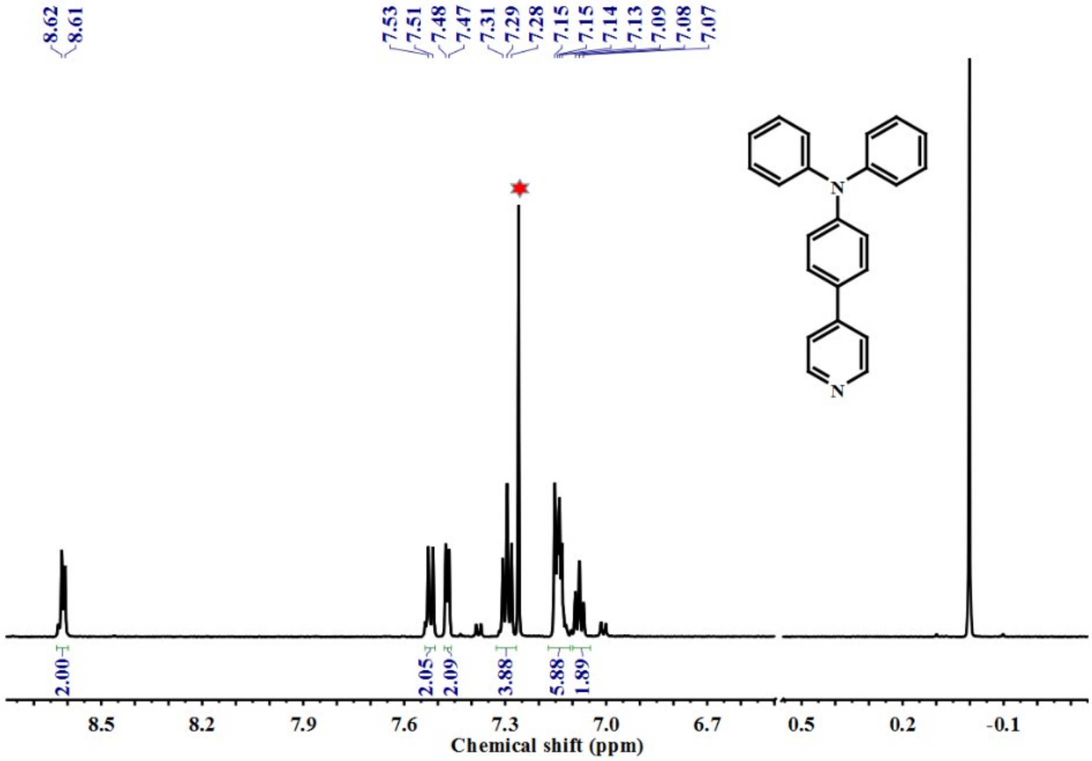

**Figure S1.** $^{1}$H NMR Spectra of TPA-Py.

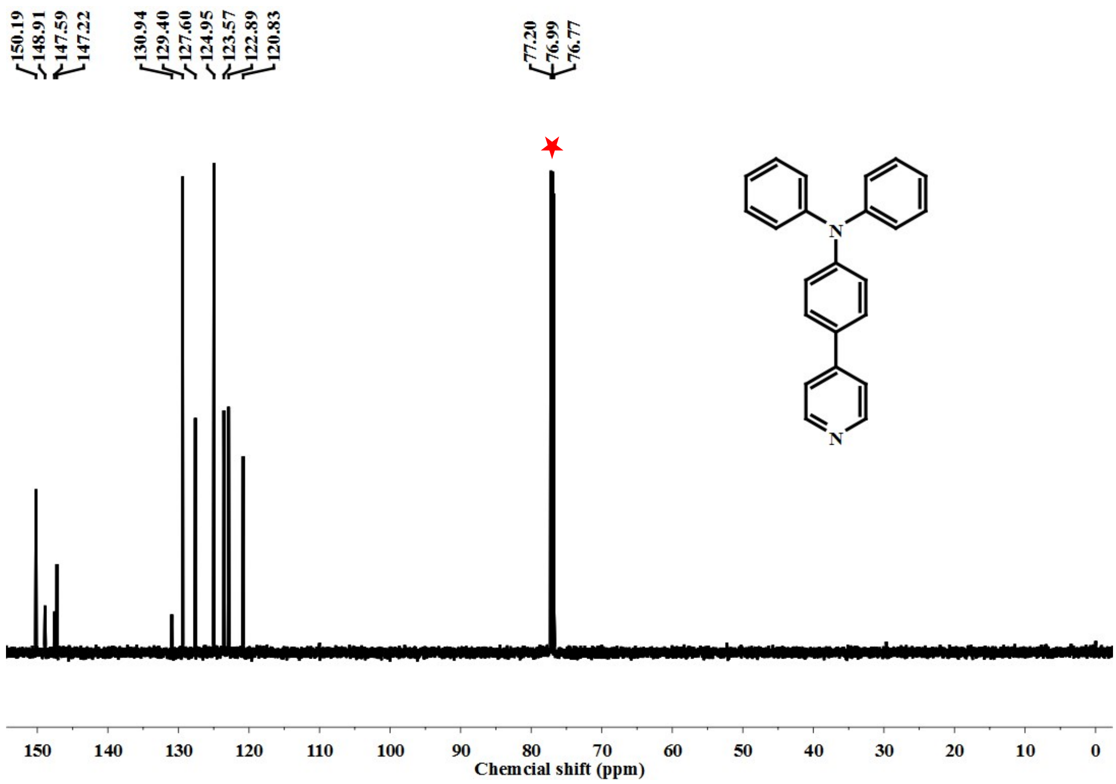

**Figure S2.** $^{13}$C NMR Spectra of TPA-Py.

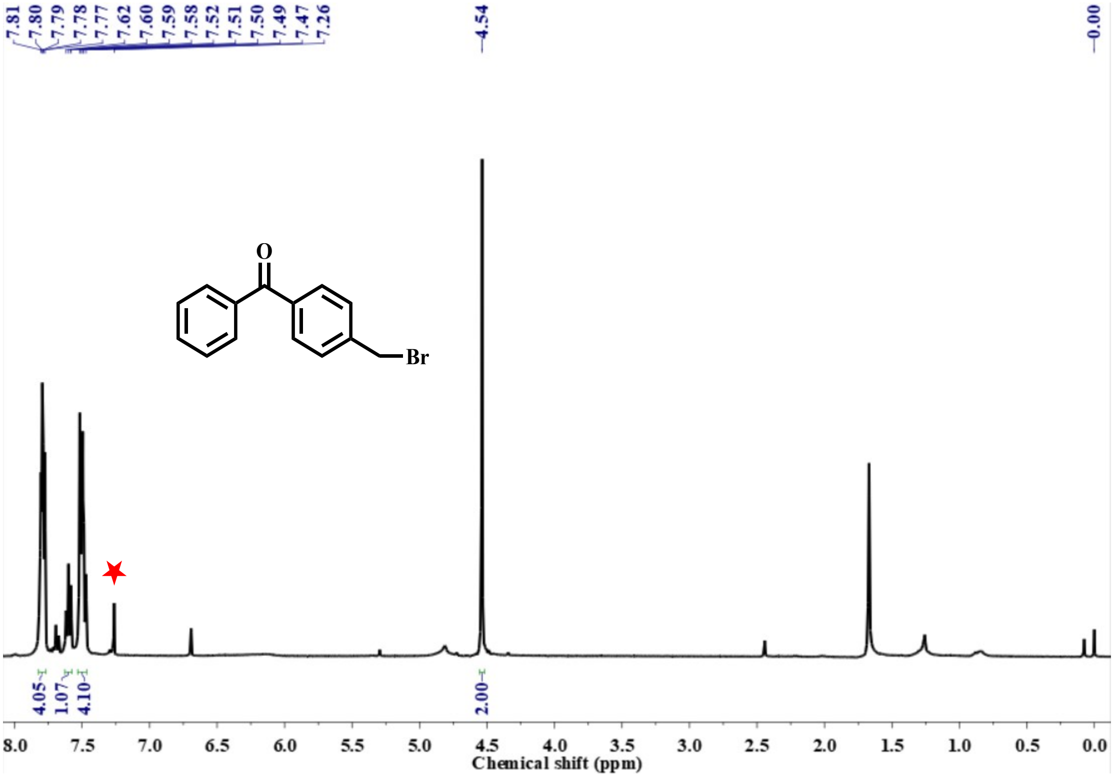


**Figure S3.** $^{1}H$ NMR Spectra of BP-Me-Br.

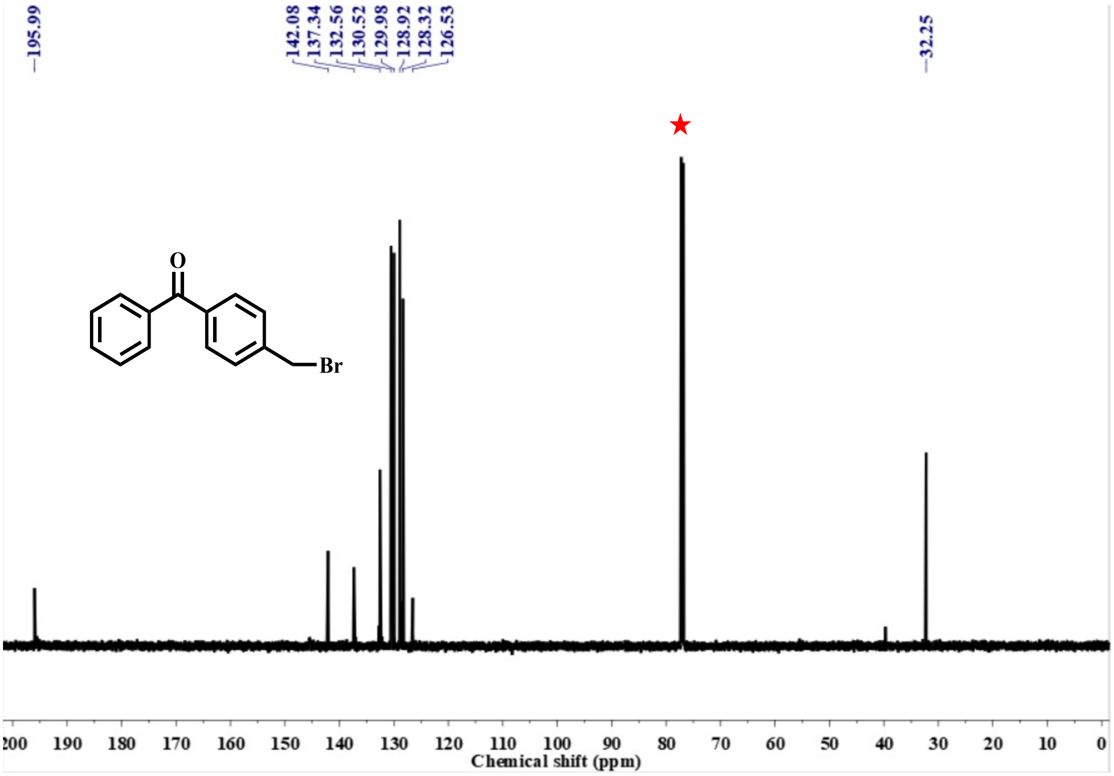


**Figure S4.** $^{13}C$ NMR Spectra of BP-Me-Br.

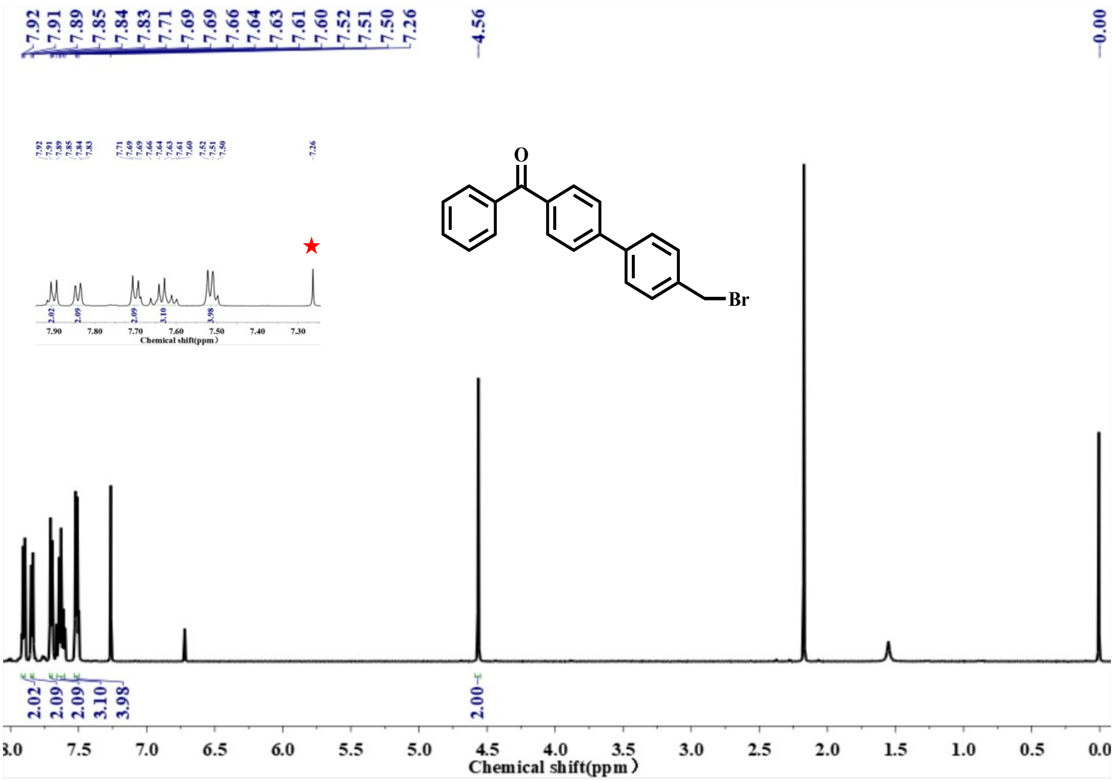


**Figure S5.** $^{1}H$ NMR Spectra of BP-Ph-Me-Br.

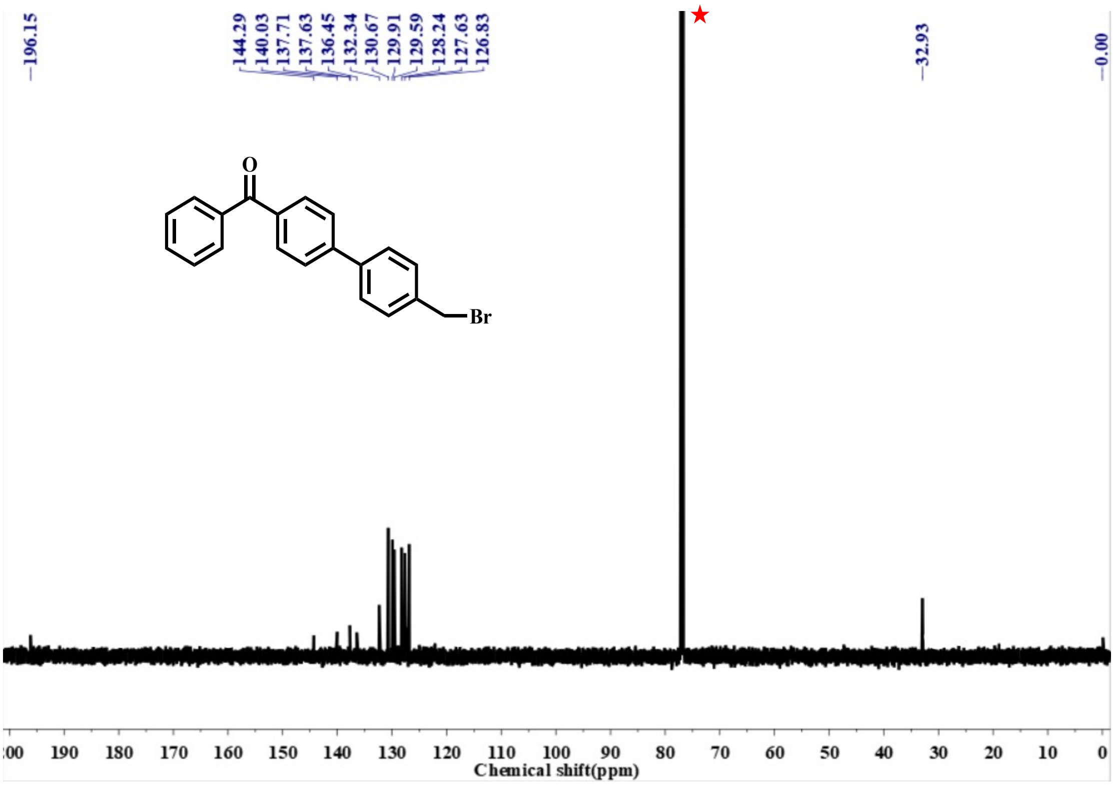


**Figure S6.** $^{13}C$ NMR Spectra of BP-Ph-Me-Br.

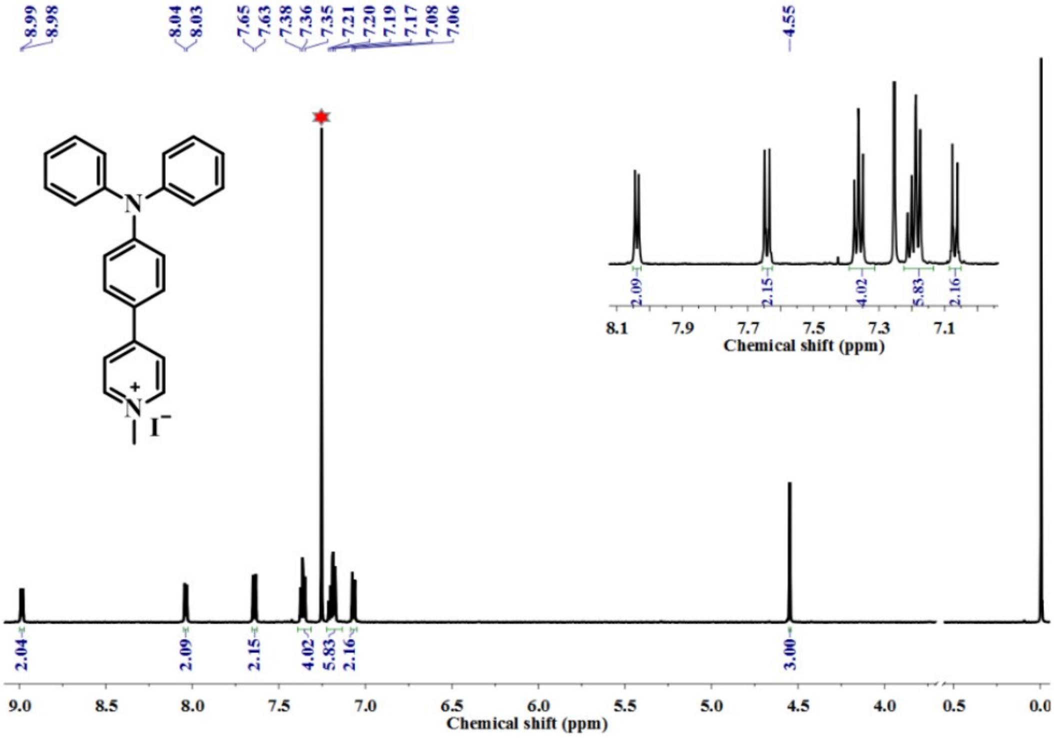


**Figure S7.** $^{1}$H NMR Spectra of TPA-Pyr-Me

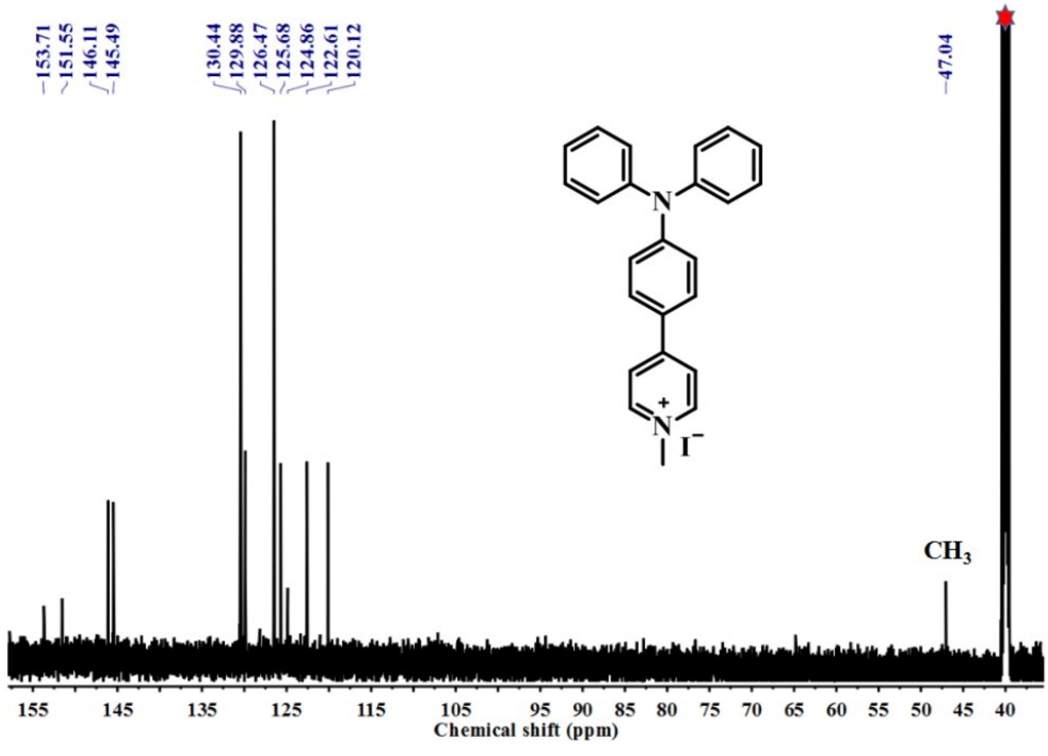


**Figure S8.** $^{13}$C NMR Spectra of TPA-Pyr-Me.

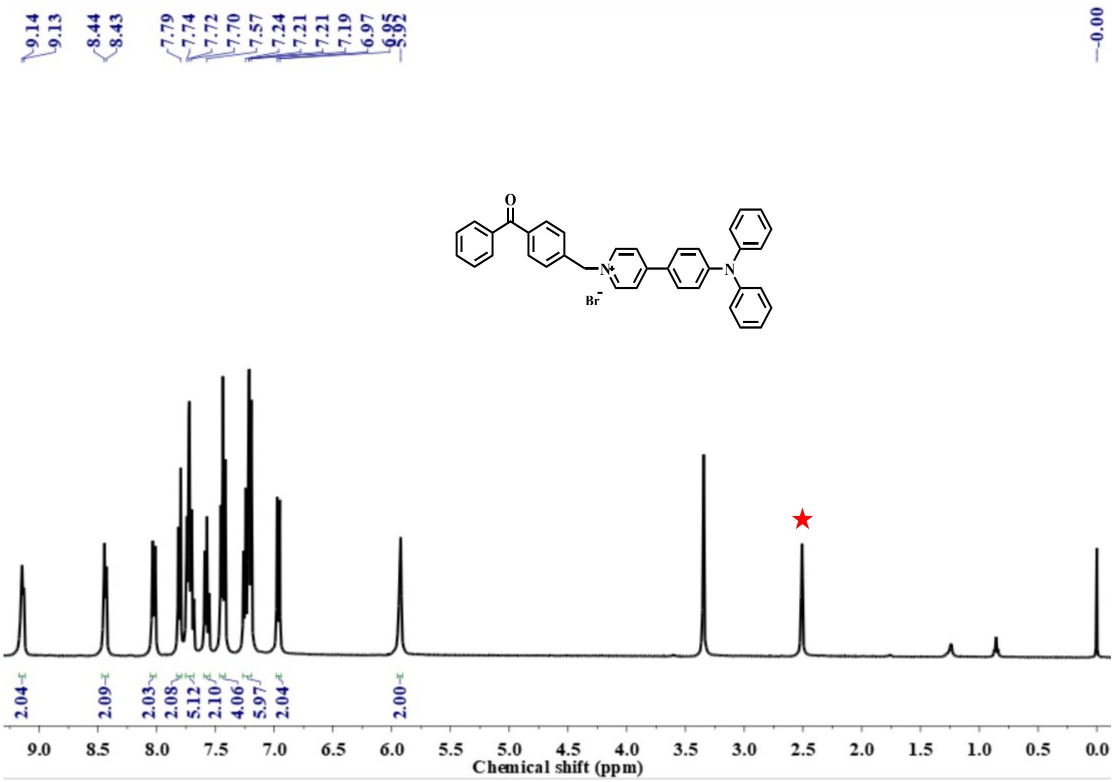

**Figure S9.** $^1H$ NMR Spectra of TPA-Pyr-BP.

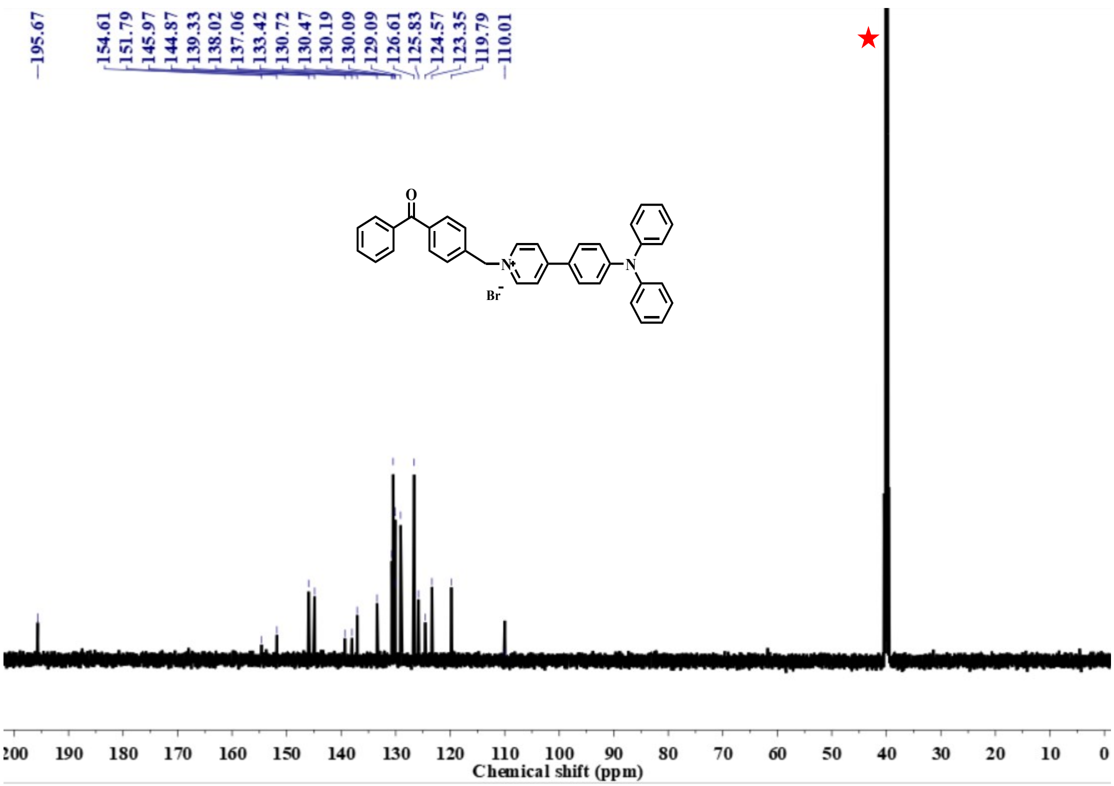

**Figure S10.** $^{13}C$ NMR Spectra of TPA-Pyr-BP.

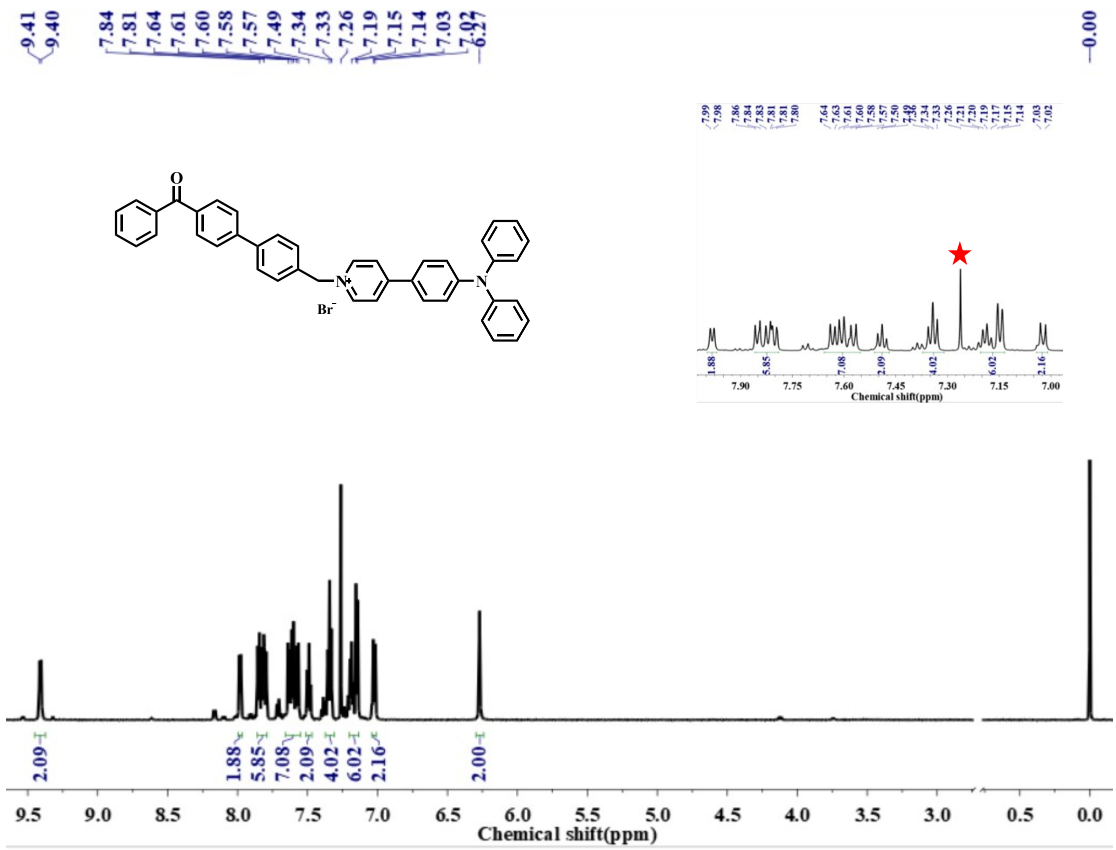


**Figure S11.** $^{1}$H NMR Spectra of TPA-Pyr-Ph-BP.

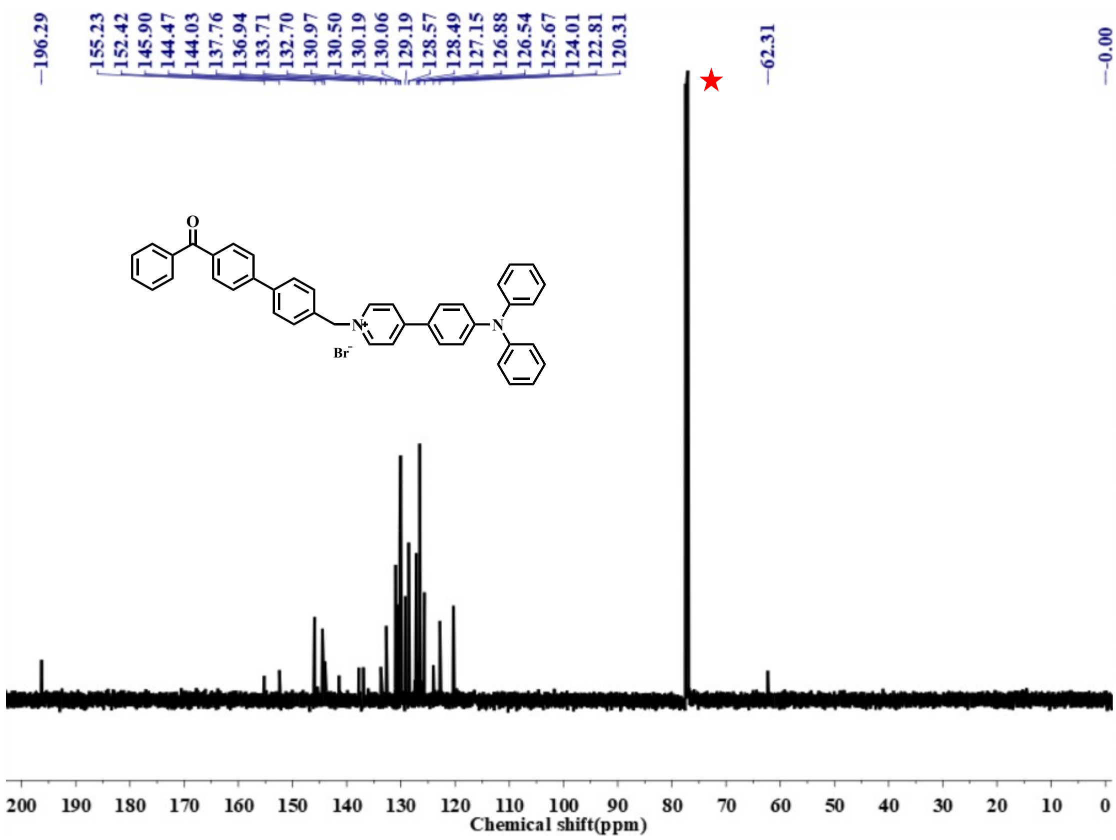


**Figure S12.** $^{13}$C NMR Spectra of TPA-Pyr-Ph-BP.

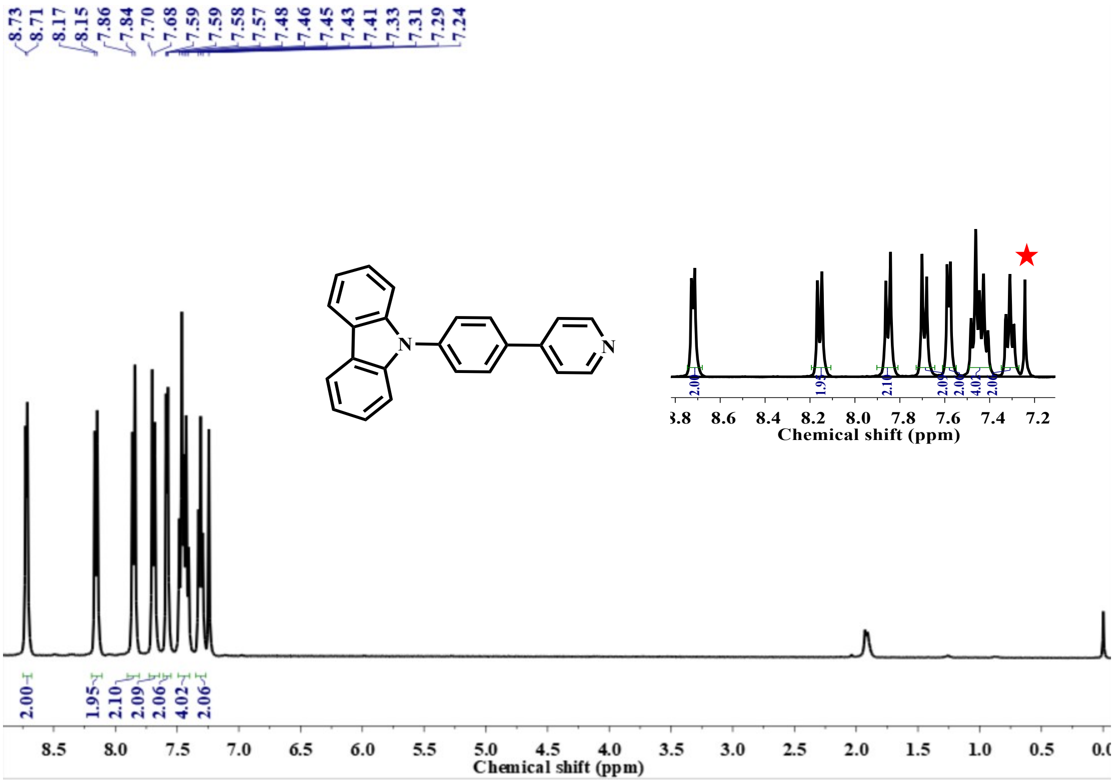


**Figure S13.** $^{1}$H NMR Spectra of CZ-Py.

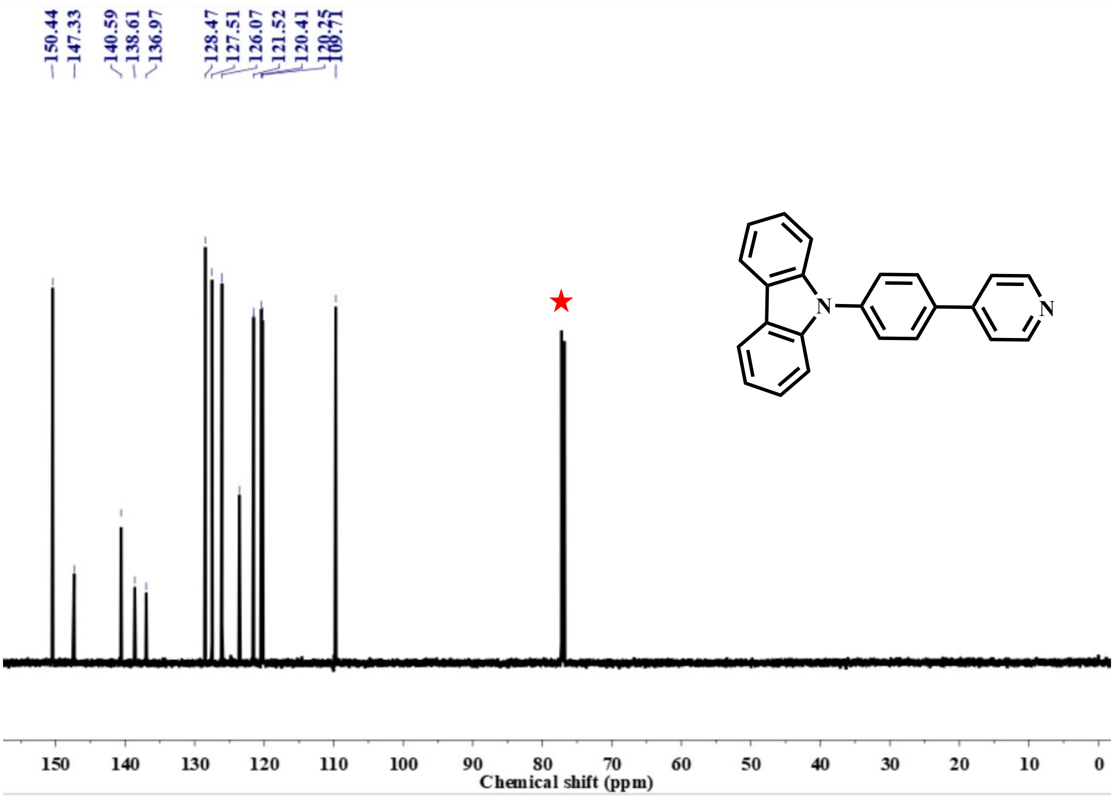


**Figure S14.** $^{13}$C NMR Spectra of CZ-Py.

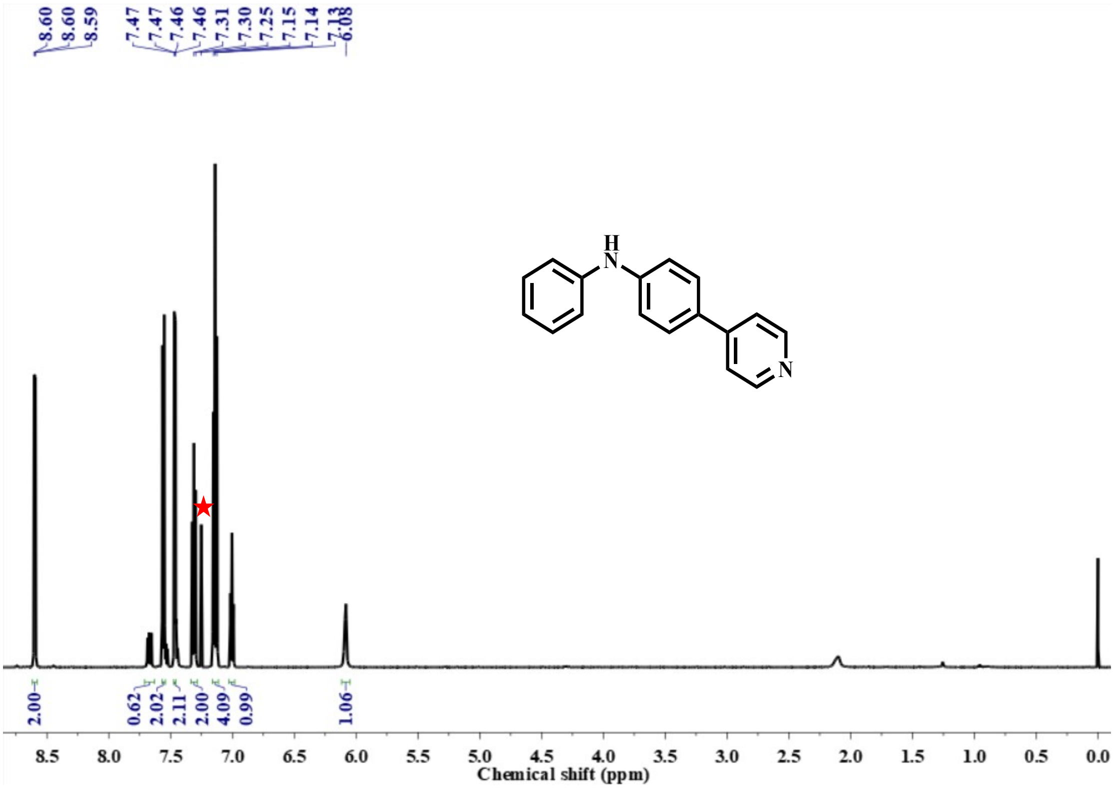


**Figure S15.** $^{1}H$ NMR Spectra of DPA-Py.

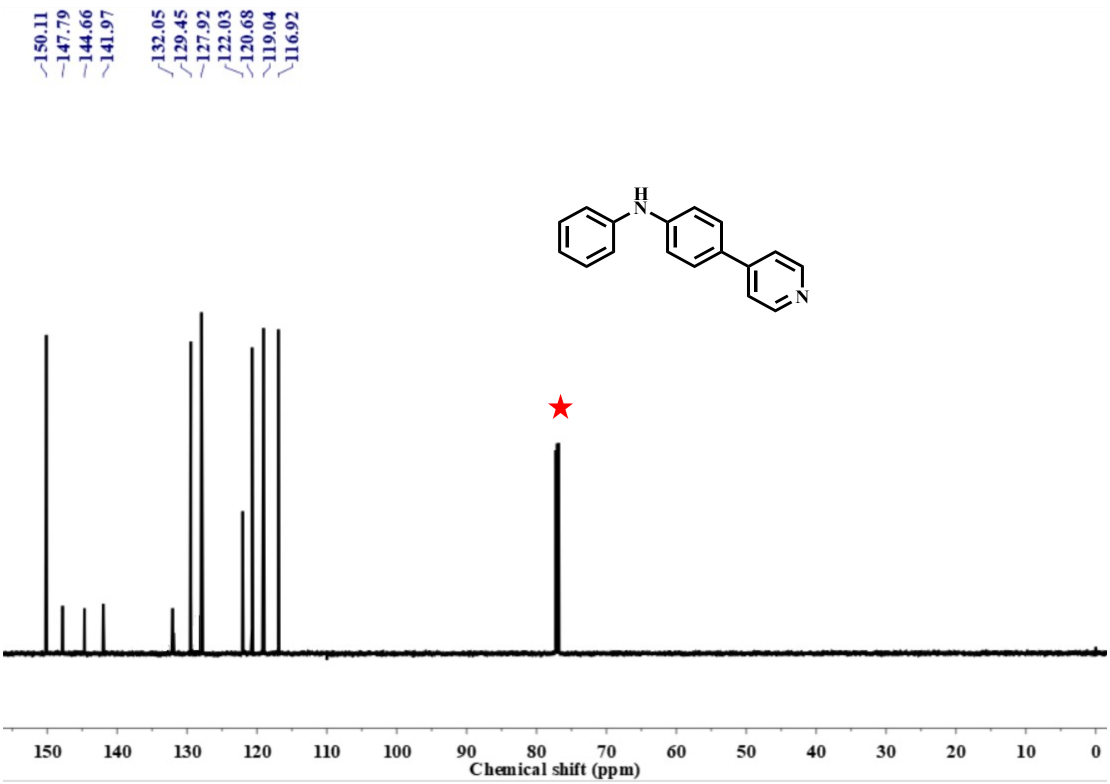


**Figure S16** $^{13}C$ NMR Spectra of DPA-Py.

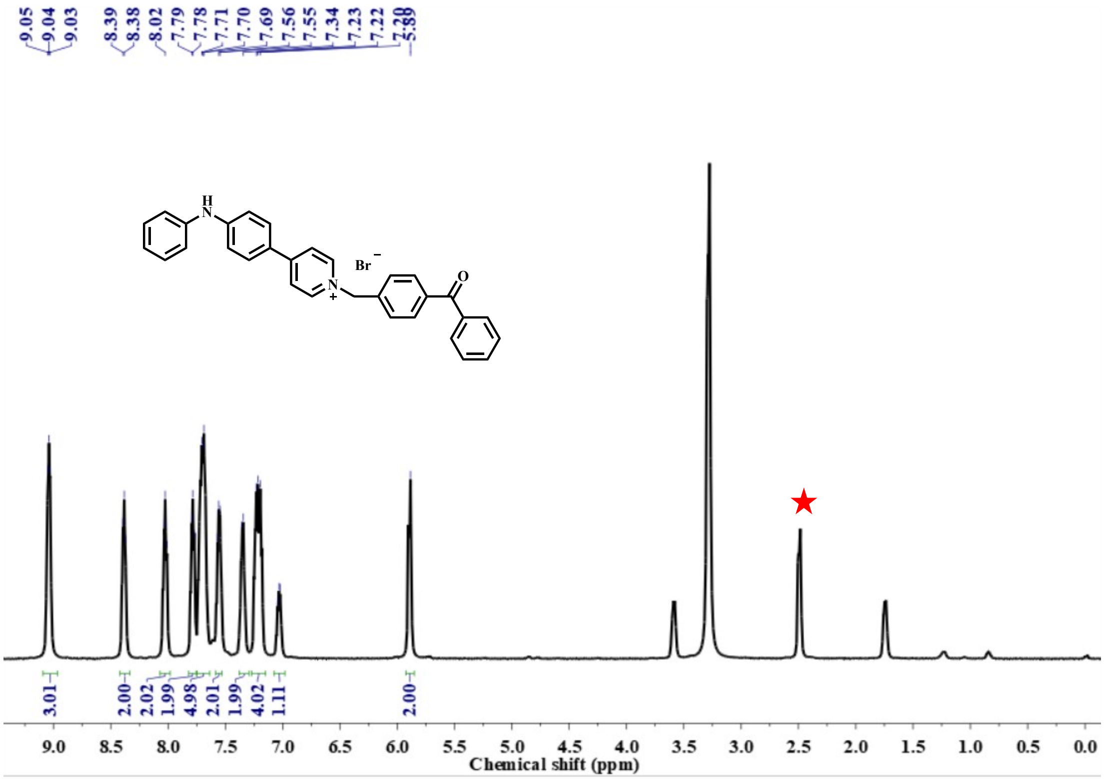


**Figure S17.** $^{1}$H NMR Spectra of DPA-Pyr-BP.

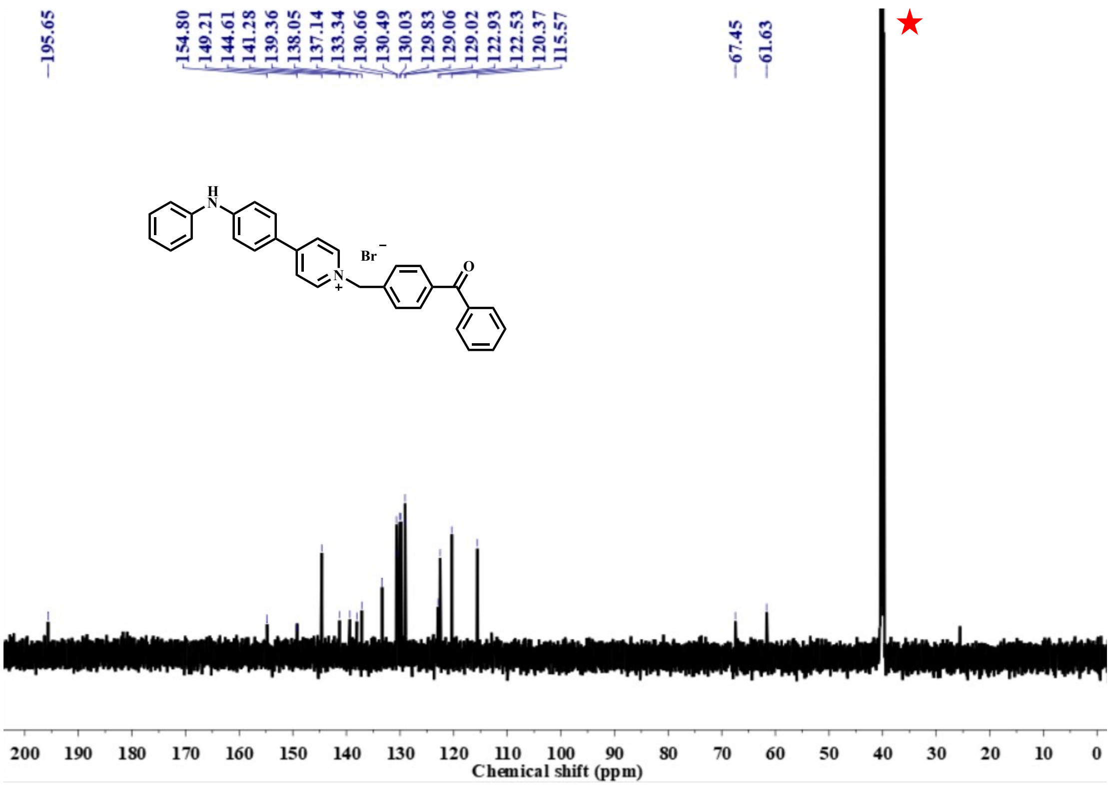


**Figure S18.** $^{13}$C NMR Spectra of DPA-Pyr-BP.

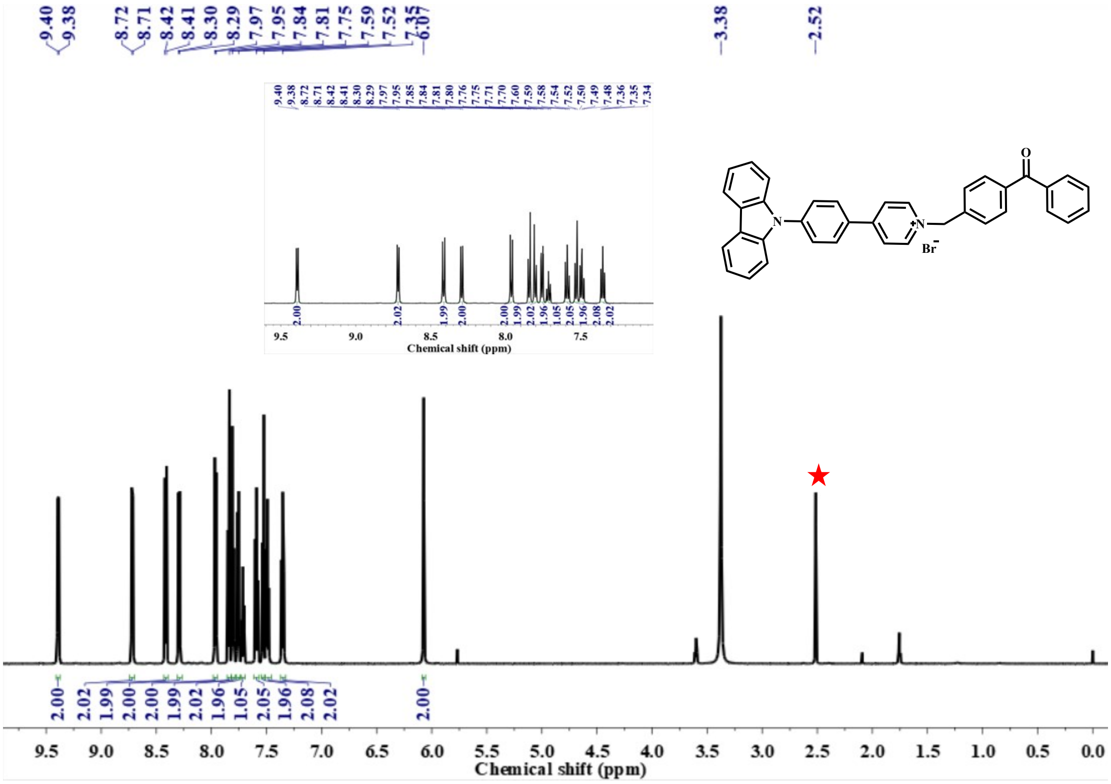

**Figure S19.** $^{1}$H NMR Spectra of CZ-Pyr-BP.

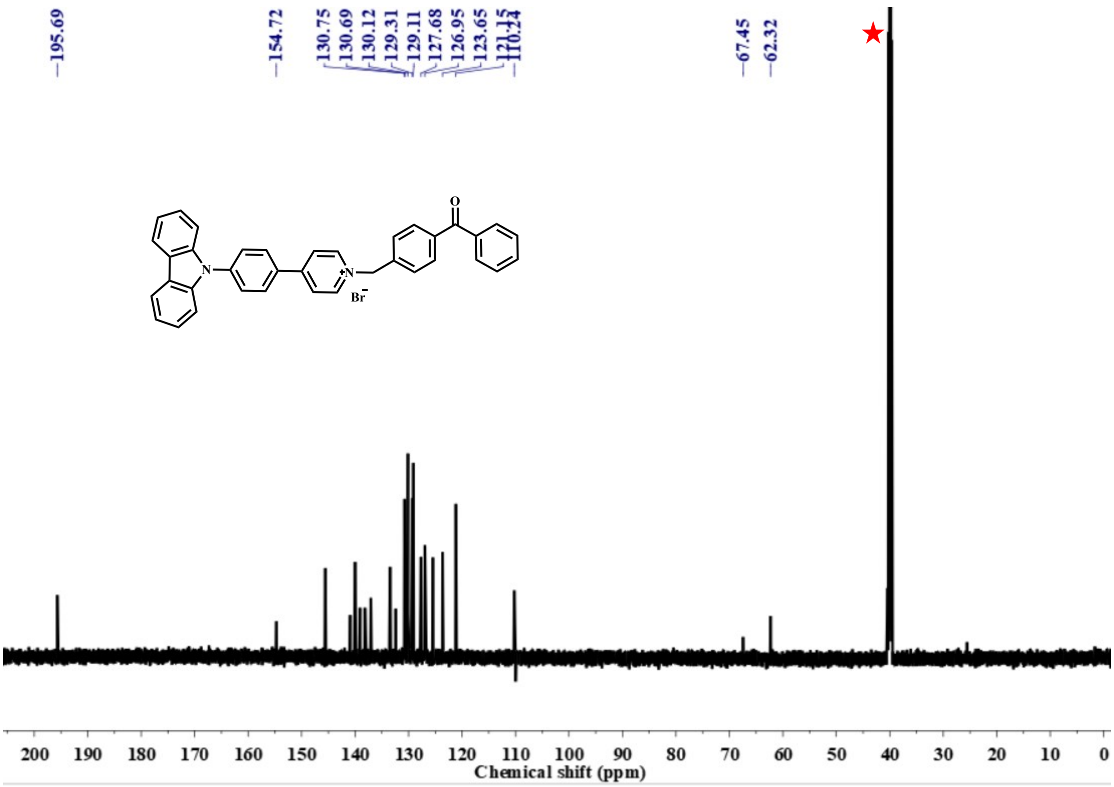

**Figure S20.** $^{13}$C NMR Spectra of CZ-Pyr-BP.

## 4. UV and PL spectra of Compounds.

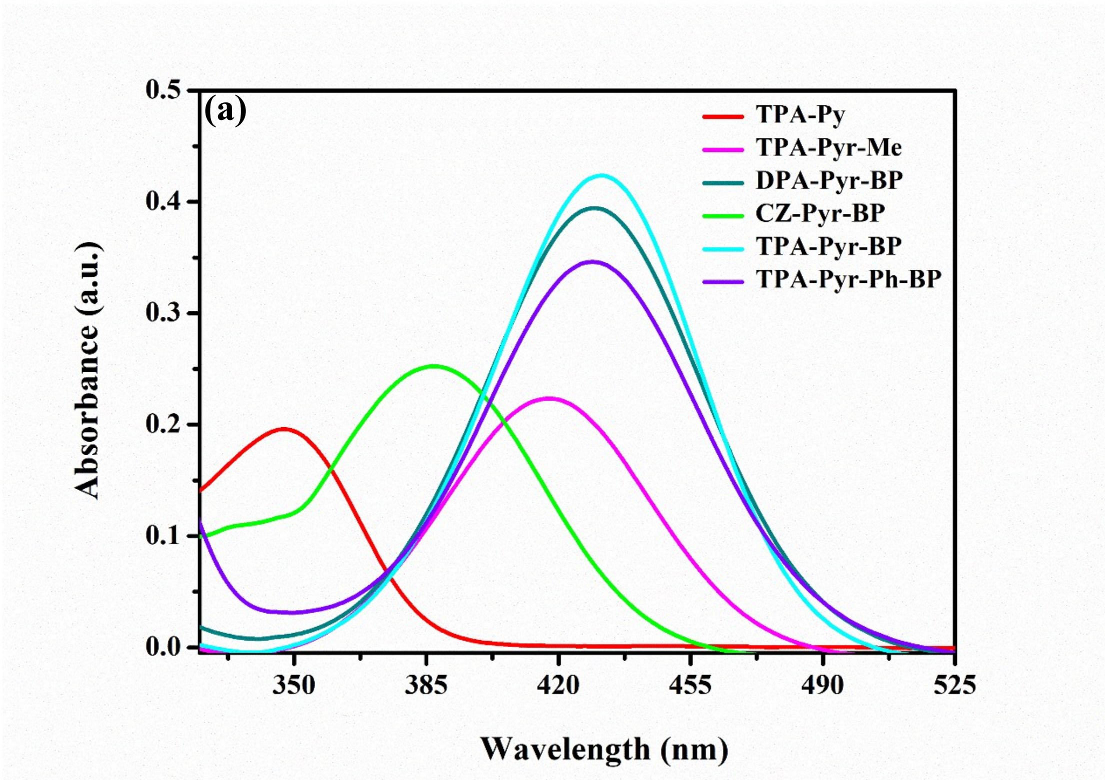


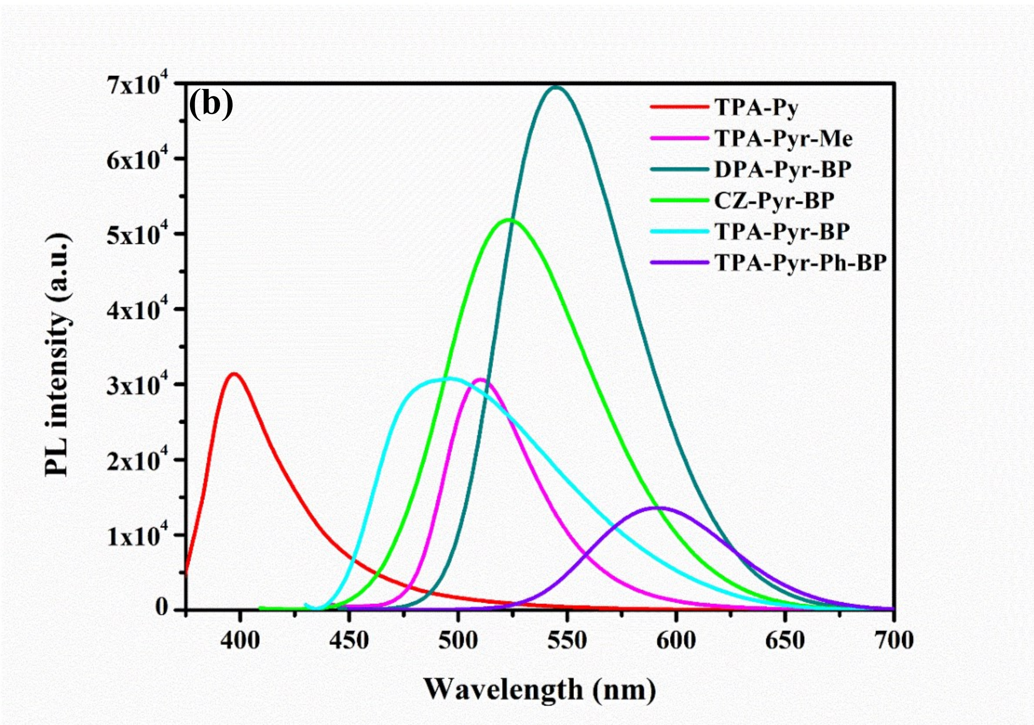


**Figure S21.** (a) UV spectra of TPA-Py, TPA-Pyr-Me, DPA-Pyr-BP, CZ-Pyr-BP, TPA-Pyr-BP and TPA-Pyr-Ph-BP in DMSO (10 μM, respectively), (b) PL spectra of TPA-Py, TPA-Pyr-Me, DPA-PYr-BP, CZ-Pyr-BP, TPA-Pyr-BP and TPA-Pyr-Ph-BP in solid state ($\lambda_{ex}$ = 347, 418, 429, 386, 430 and 428 nm, respectively).

## 5. Study on ACQ or AIE properties of compounds.

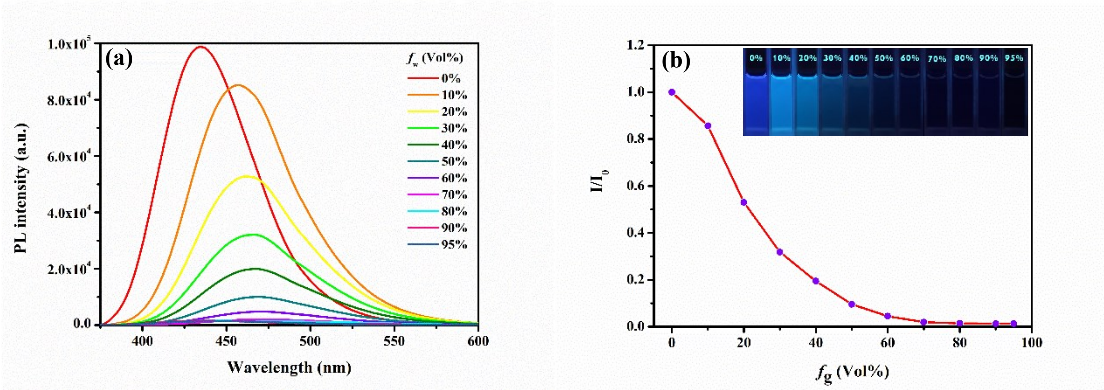


**Figure S22.** (a) PL spectra of TPA-Py in glycerol and methanol mixture with different glycerol fractions (concentration: 10 μM, $\lambda_{ex}$ = 347 nm). (b) The plot of the emission maximum of TPA-Py. Inset shown the photographs in different glycerol fractions under illumination at 365 nm.

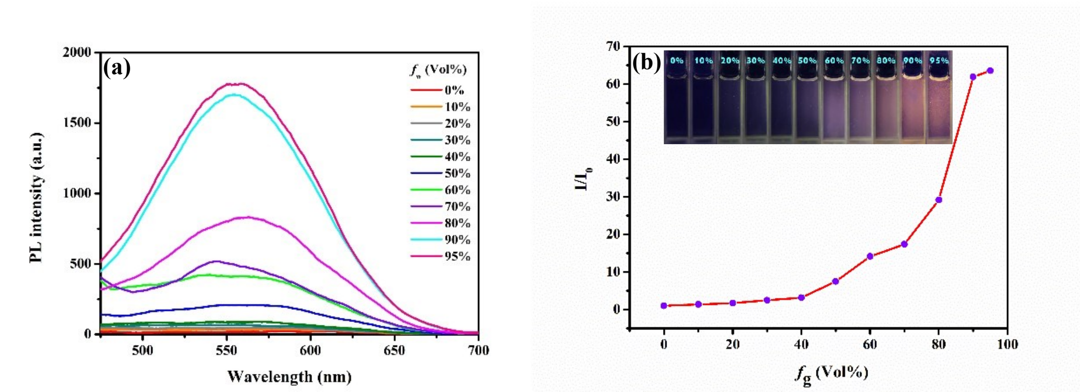


**Figure S23.** (a) PL spectra of TPA-Pyr-Me in glycerol and methanol mixture with different glycerol fractions (concentration: 10 μM, $\lambda_{ex}$ = 418 nm). (b) The plot of the emission maximum of TPA-Pyr-Me. Inset shown the photographs in different glycerol fractions under illumination at 365 nm.

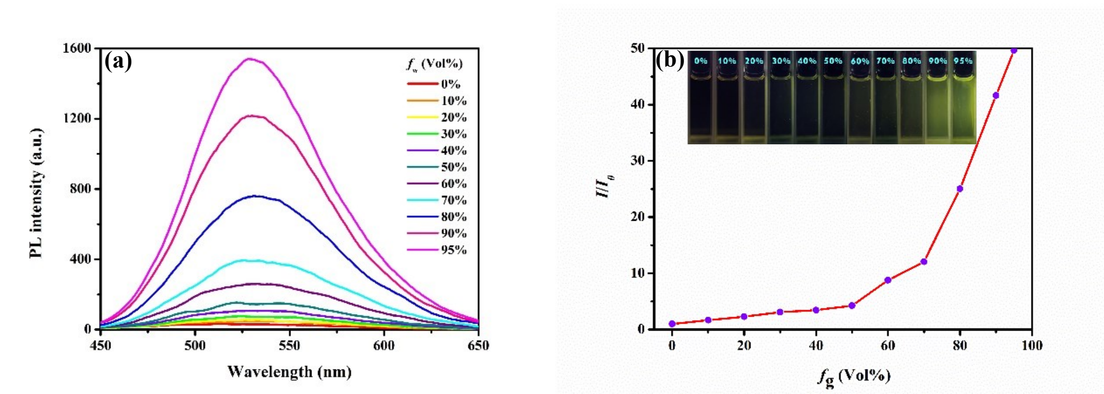


**Figure S24.** (a) PL spectra of DPA-Pyr-BP in glycerol and methanol mixture with different glycerol fractions (concentration: 10 μM, $\lambda_{ex}$ = 429 nm). (b) The plot of the emission maximum of DPA-Pyr-BP. Inset shown the photographs in different glycerol fractions under illumination at 365 nm.

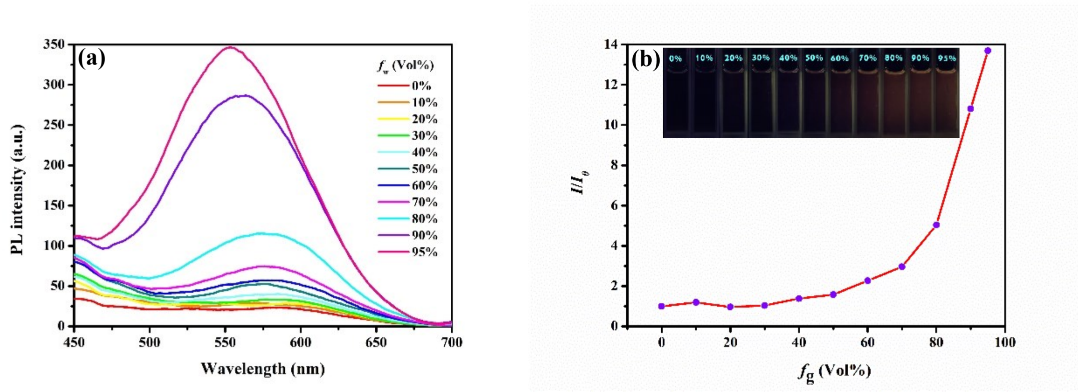


**Figure S25.** (a) PL spectra of CZ-Pyr-BP in glycerol and methanol mixture with different glycerol fractions (concentration: 10 μM, $\lambda_{ex}$ = 386 nm). (b) The plot of the emission maximum of CZ-Pyr-BP. Inset shown the photographs in different glycerol fractions under illumination at 365 nm.

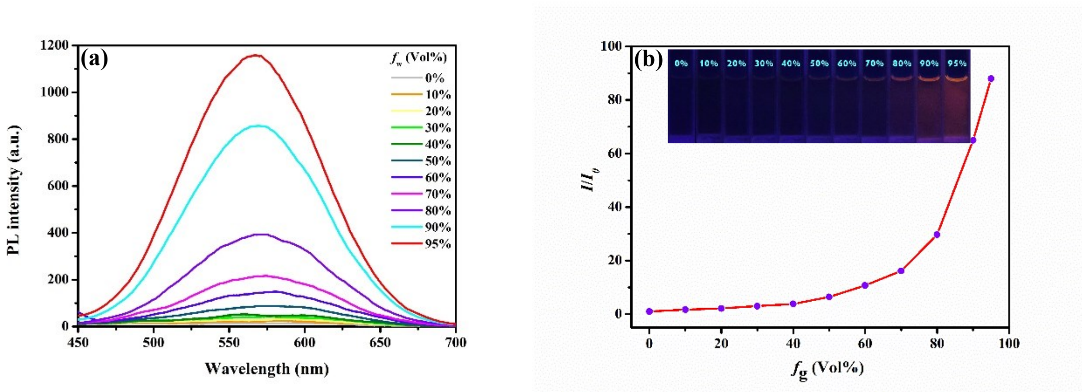


**Figure S26.** (a) PL spectra of TPA-Pyr-BP in glycerol and methanol mixture with different glycerol fractions (concentration: 10 μM, $\lambda_{ex}$ = 430 nm). (b) The plot of the emission maximum of TPA-Pyr-BP. Inset shown the photographs in different glycerol fractions under illumination at 365 nm.

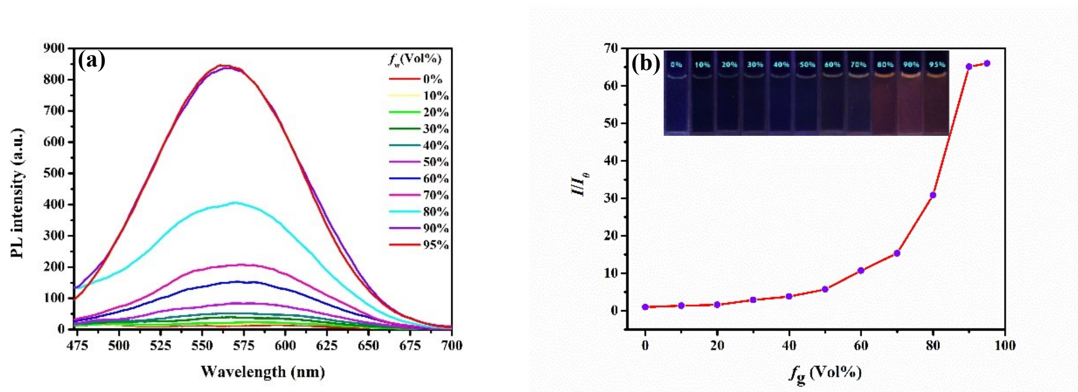


**Figure S27.** (a) PL spectra of TPA-Pyr-Ph-BP in glycerol and methanol mixture with different glycerol fractions (concentration: 10 μM, $\lambda_{ex}$ = 428 nm). (b) The plot of the emission maximum of TPA-Pyr-Ph-BP. Inset shown the photographs in different glycerol fractions under illumination at 365 nm.

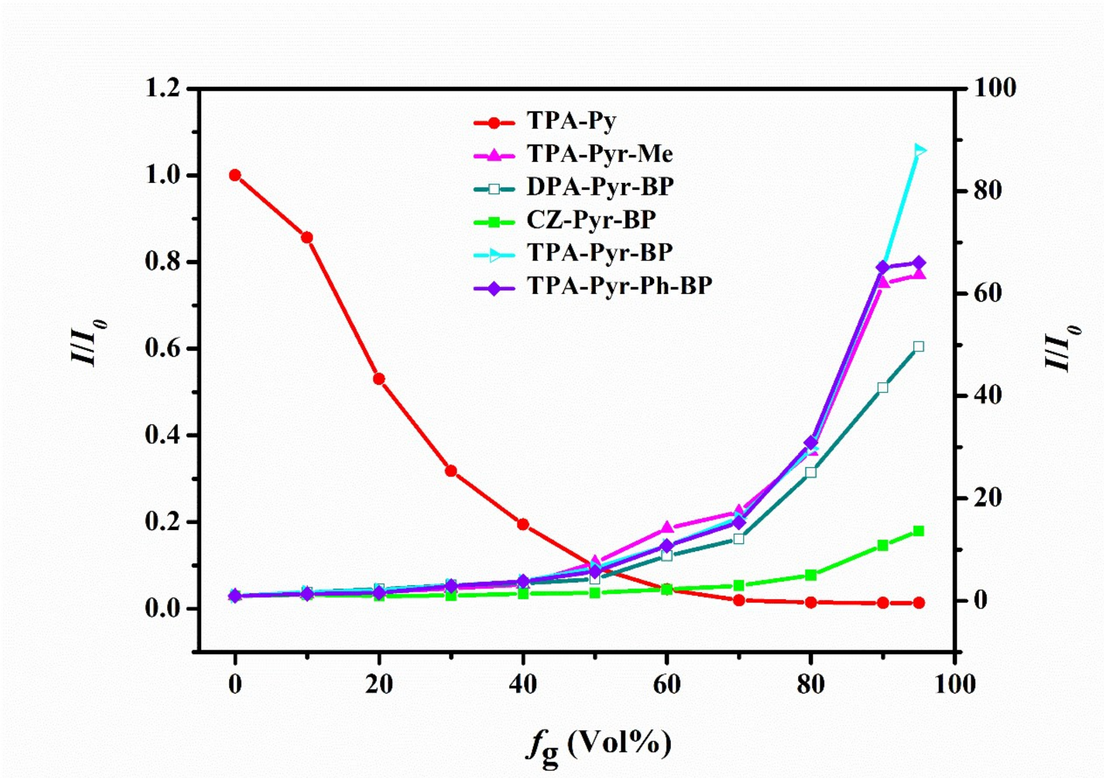


**Figure 28.** The plot of the emission maximum of TPA-Py, TPA-Pyr-Me, DPA-PYr-BP, CZ-Pyr-BP, TPA-Pyr-BP and TPA-Pyr-Ph-BP in glycerol and methanol mixture with different glycerol fractions (concentration: 10 μM, λex = 347, 418, 429, 386, 430, 428 nm, respectively).

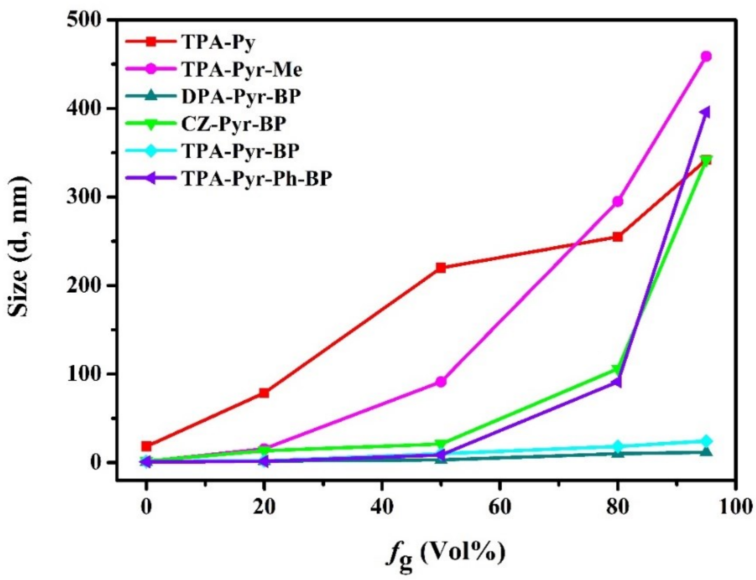


**Figure S29.** The plot of the particle size of TPA-Py, TPA-Pyr-Me, DPA-PYr-BP, CZ-Pyr-BP, TPA-Pyr-BP and TPA-Pyr-Ph-BP in glycerol and methanol mixture with different glycerol fractions (0%, 20%, 50%, 80% and 95%).

**6. Mechanoluminescent properties of compounds.**

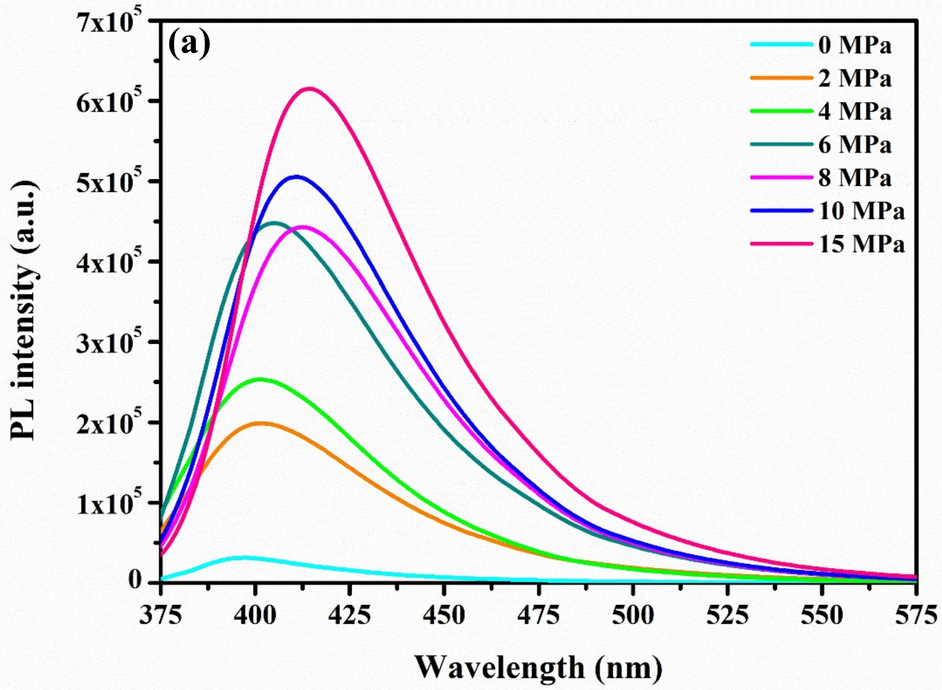


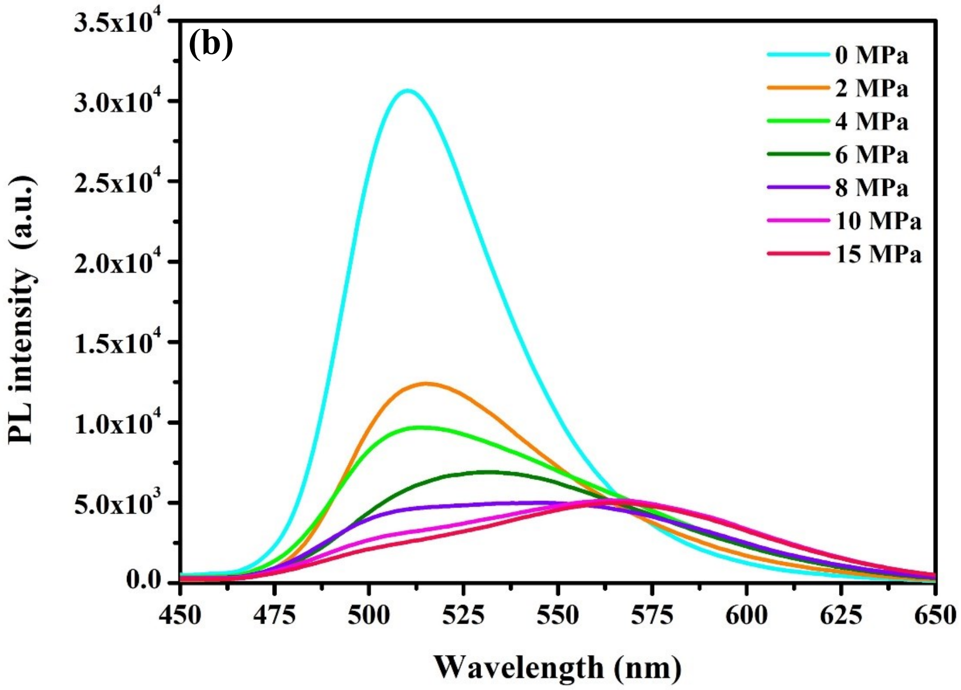

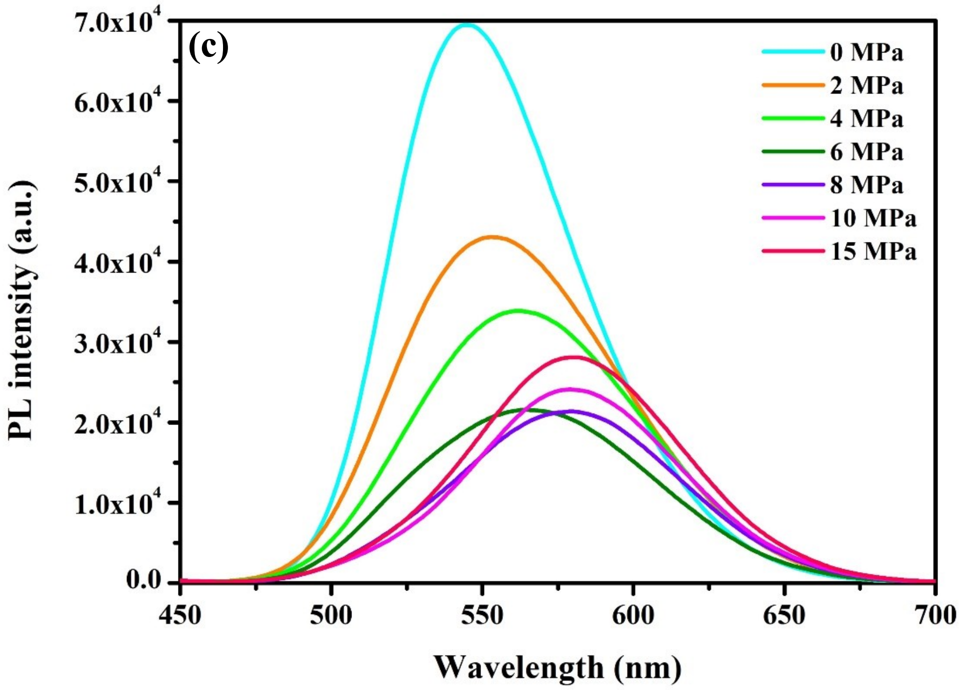
(c)
0 MPa
2 MPa
4 MPa
6 MPa
8 MPa
10 MPa
15 MPa
PL intensity (a.u.)
7.0x10^4
6.0x10^4
5.0x10^4
4.0x10^4
3.0x10^4
2.0x10^4
1.0x10^4
0.0
450
500
550
600
650
700
Wavelength (nm)

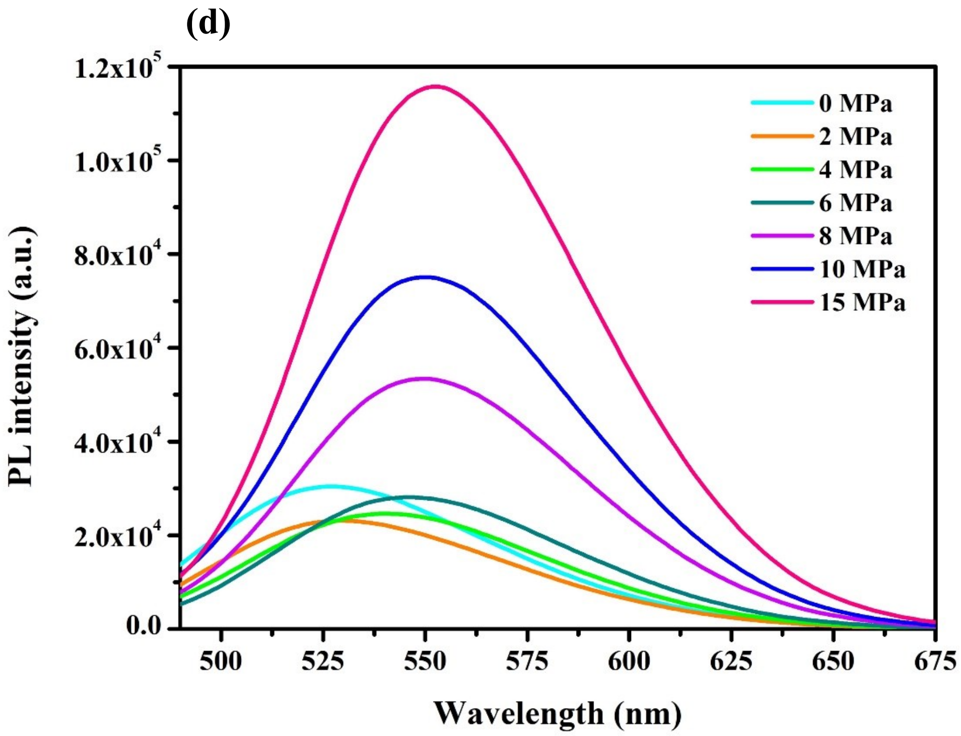
(d)
0 MPa
2 MPa
4 MPa
6 MPa
8 MPa
10 MPa
15 MPa
PL intensity (a.u.)
1.2x10^5
1.0x10^5
8.0x10^4
6.0x10^4
4.0x10^4
2.0x10^4
0.0
500
525
550
575
600
625
650
675
Wavelength (nm)

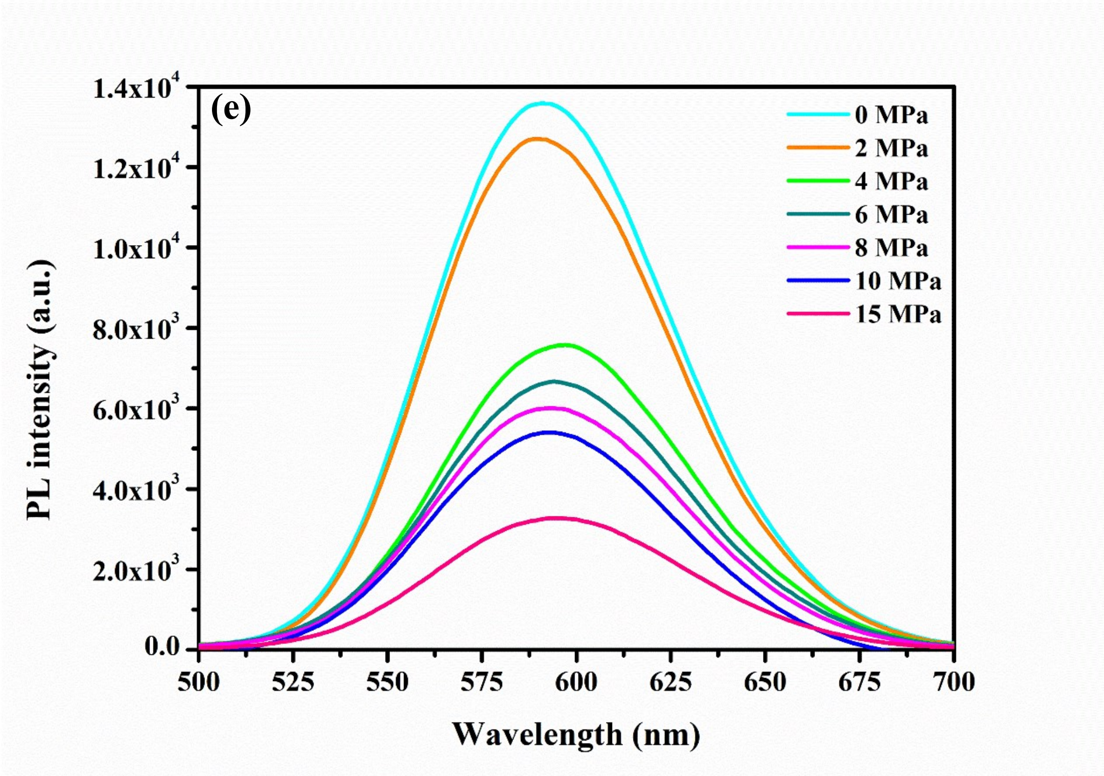


**Figure S30.** (a, b, c, d, e) Fluorescence emission spectra of TPA-Py, TPA-Pyr-Me, DPA-Pyr-BP, CZ-Pyr-BP and TPA-Pyr-Ph-BP under different pressures ($\lambda_{ex}$ = 347, 418, 429, 386 and 428 nm, respectively).

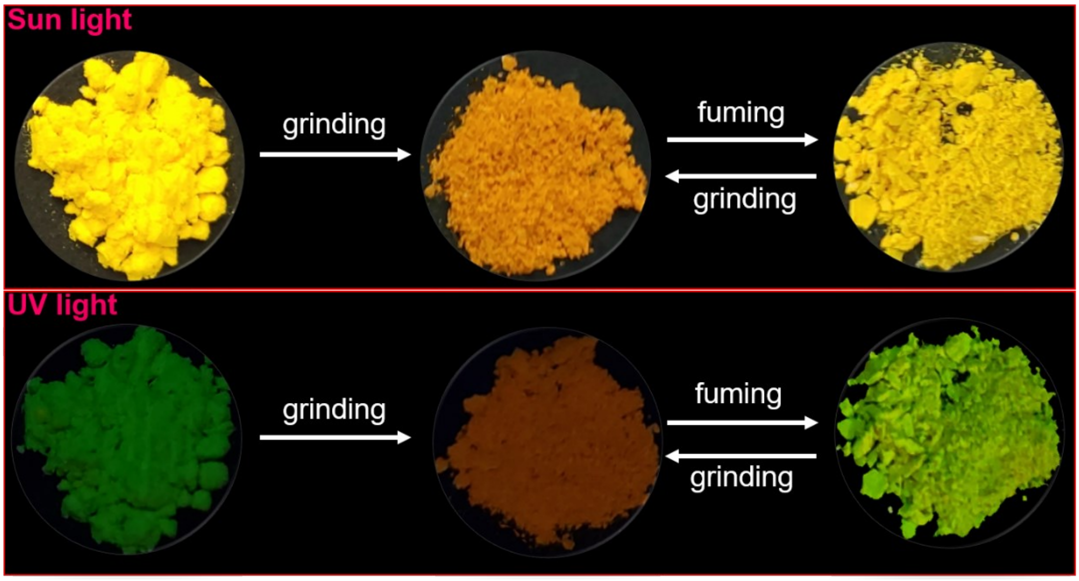


**Figure S31.** Images of reversible mechanochromic fluorescence under grinding /fuming of TPA-Pyr-Me under sun light and UV light.

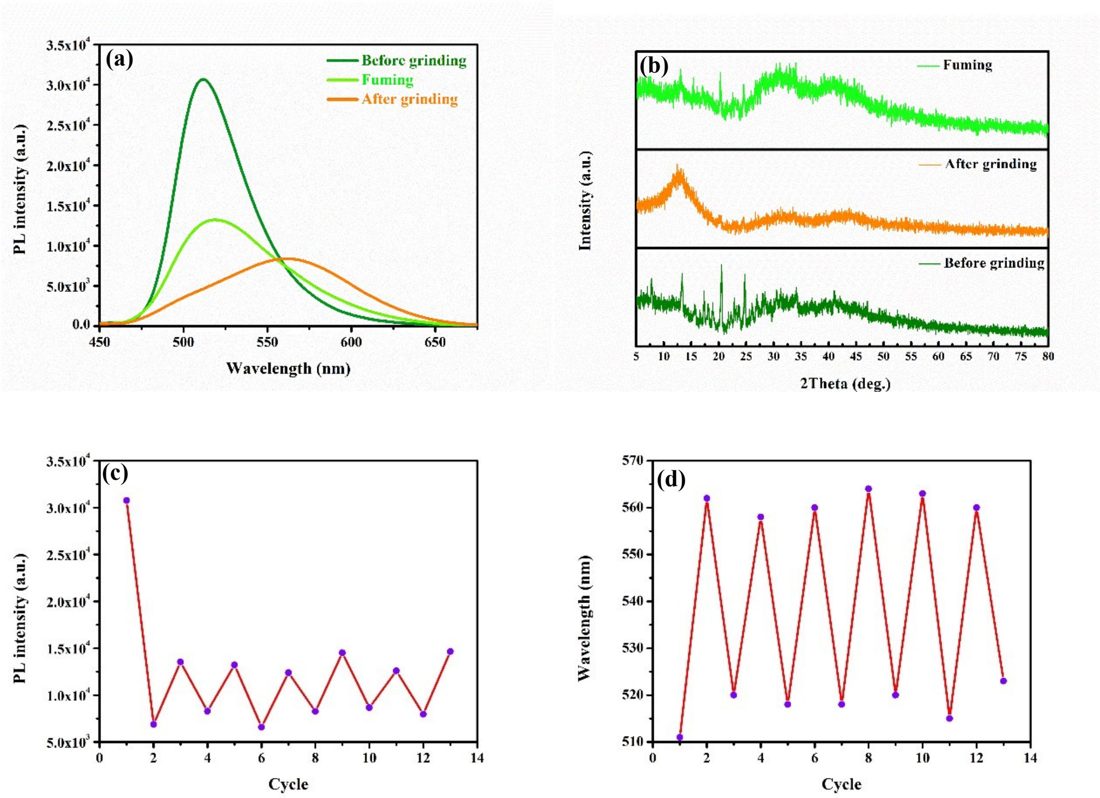


**Figure S32.** (a) Change in the emission spectrum of TPA-Pyr-Me powder by the grinding-fuming process. (b) X-ray diffraction (XRD) spectra of TPA-Pyr-Me in different aggregated states. (c, d) Repeated switching of the solid-state fluorescence of TPA-Pyr-Me by repeated grinding and fuming cycles.

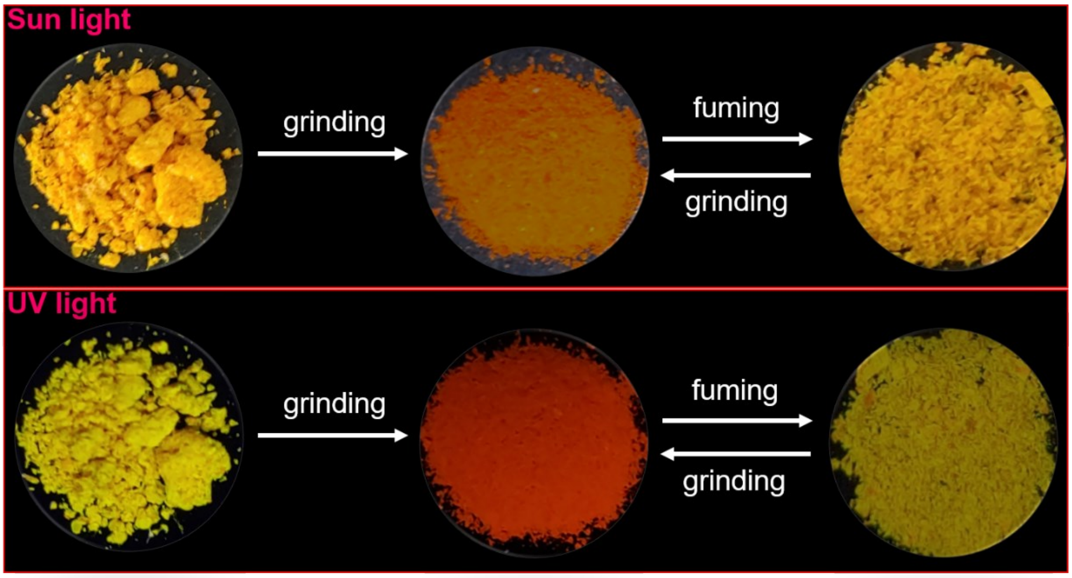


**Figure S33.** Images of reversible mechanochromic fluorescence under grinding /fuming of DPA-Pyr-BP under sun light and UV light.

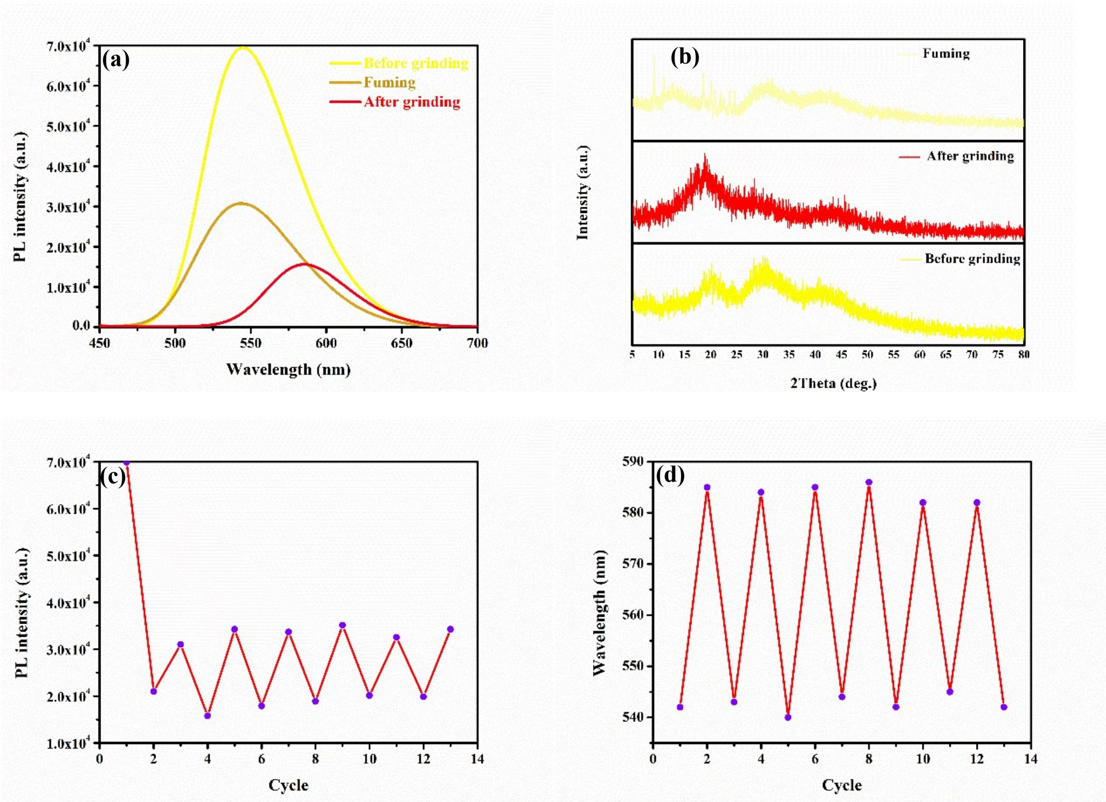


**Figure S34.** (a) Change in the emission spectrum of DPA-Pyr-BP powder by the grinding-fuming process. (b) X-ray diffraction (XRD) spectra of DPA-Pyr-BP in different aggregated states. (c, d) Repeated switching of the solid-state fluorescence of DPA-Pyr-BP by repeated grinding and fuming cycles.

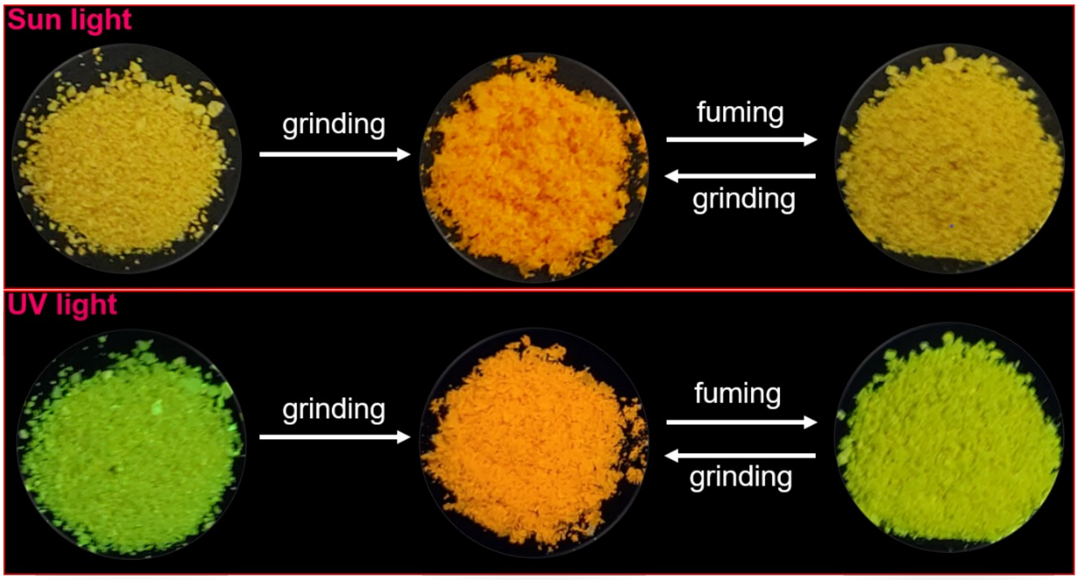


**Figure S35.** Images of reversible mechanochromic fluorescence under grinding /fuming of CZ-Pyr-BP under sun light and UV light.

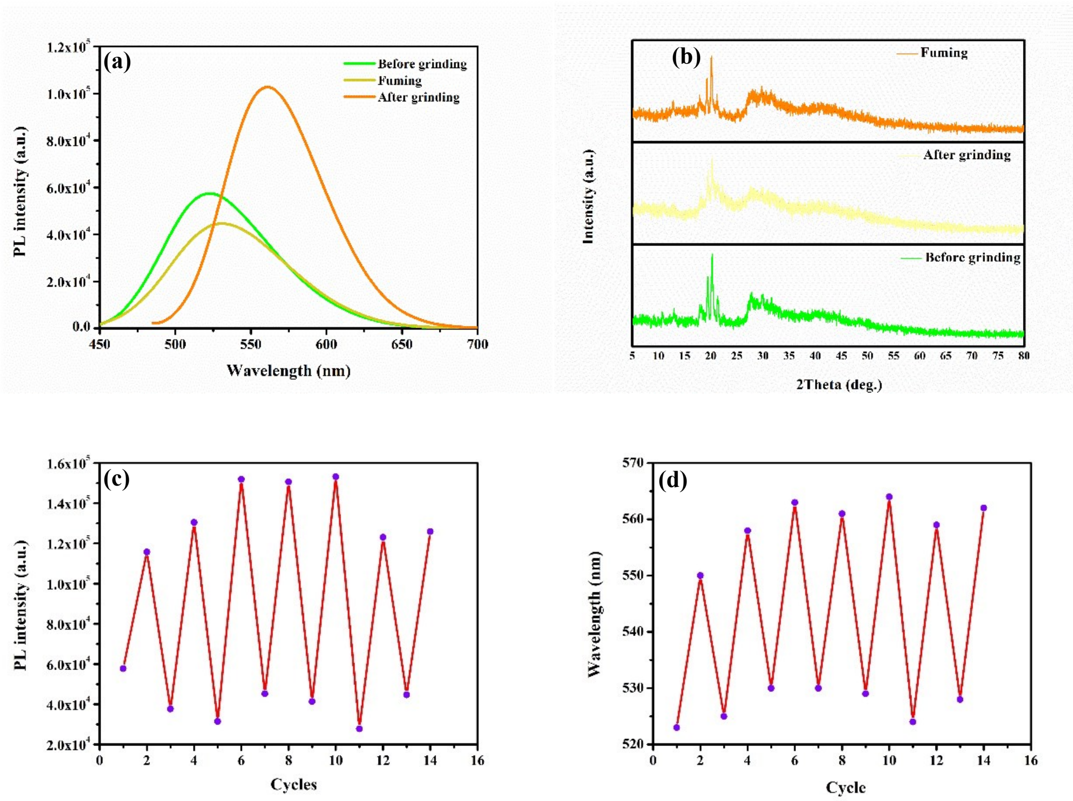


**Figure S36.** (a) Change in the emission spectrum of CZ-Pyr-BP powder by the grinding-fuming process. (b) X-ray diffraction (XRD) spectra of CZ-Pyr-BP in different aggregated states. (c, d) Repeated switching of the solid-state fluorescence of CZ-Pyr-BP by repeated grinding and fuming cycles.

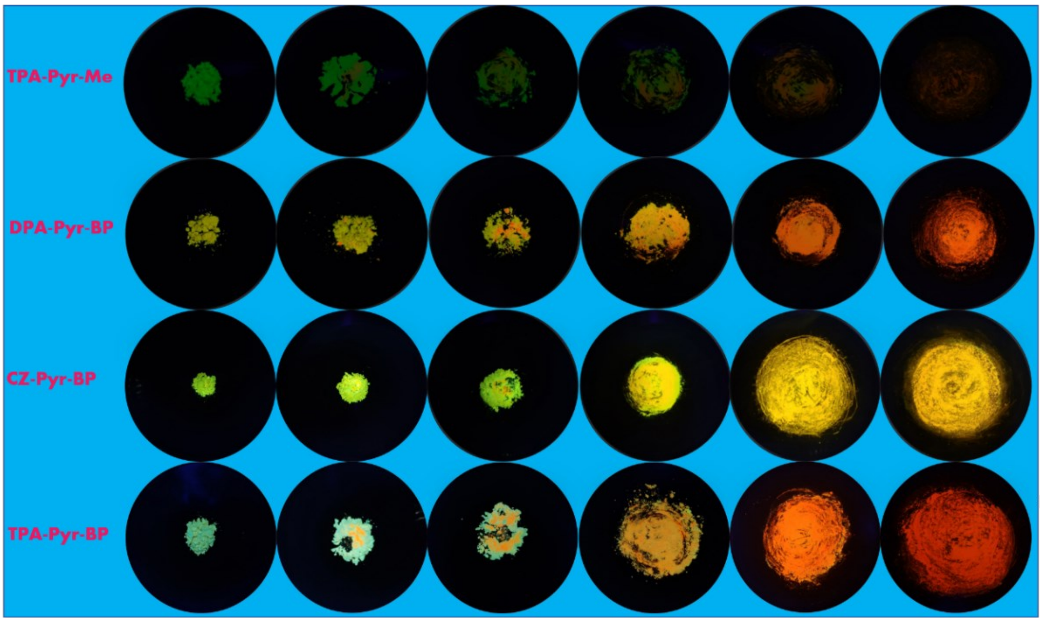


**Figure S37.** The photos of TPA-Pyr-Me, DPA-Pyr-BP, CZ-Pyr-BP and TPA-Pyr-BP in agate mortar during grinding under illumination at 365 nm.

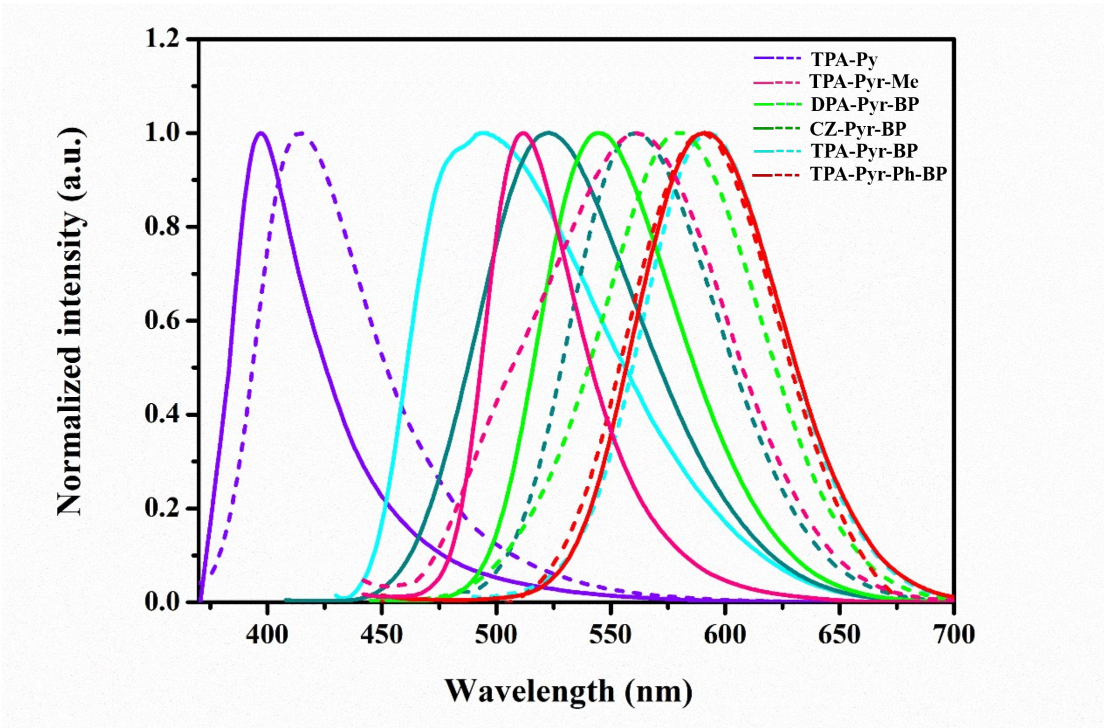


**Figure S38.** Normalized PL spectra of TPA-Py, TPA-Pyr-Me, DPA-Pyr-BP, CZ-Pyr-BP, TPA-Pyr-BP and TPA-Pyr-Ph-BP before and after grinding (the solid line represents the emission spectrum before grinding, the dotted line represents the emission spectrum after grinding).

**Table S1**. Comparison of ML properties between TPA-Pyr-BP and reported molecules.

| sample | pressure | $\lambda^a$ (nm) | $\lambda^b$ (nm) | $\Delta\lambda$ (nm) |
|---|---|---|---|---|
| DAAD[1] | 5.08 GPa | 550 | 620 | 70 |
| (S, S)-1[2] | 2.41 GPa | 450 | 528 | 78 |
| ON-TPA[3] | 2.1 GPa | 552 | 598 | 46 |
| CN-DSB[4] | 0.75 GPa | 445 | 518 | 73 |
| DMCS-TPA[5] | 10 MPa | 525 | 589 | 74 |
| Cz-CNDSB[6] | 9.21 GPa | 529 | 684 | 155 |
| TPE[7] | 5.3 GPa | 448 | 467 | 19 |
| TPA-Pyr-BP | 0.2 MPa | 488 | 590 | 102 |

[a]emission wavelength of the initial sample, [b]emission wavelength under pressure stimulation.

## 7. Single crystal date of TPA-Pyr-BP and CZ-Pyr-BP .

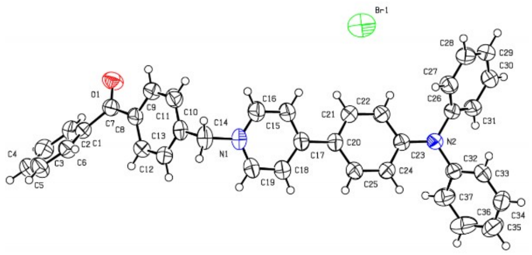

**Figure S39.** Single crystal X-ray structure of TPA-Pyr-BP.

**Table S2**. Crystal data and structure refinement for TPA-Pyr-BP.

| | |
|---|---|
| Empirical formula | $C_{37}H_{29}N_2OBr$ |
| Formula weight | 597.52 |
| Temperature | 294 K |
| Wavelength | 1.54184 |
| Bond precision | C-C = 0.0048 Å |
| Unit cell dimensions | a = 9.1969(3) Å alpha = 90 deg |
| | b = 17.9586(4) Å beta = 100.438(3) deg |
| | c = 20.7468(6) Å gamma = 90 deg |
| Volume | 3369.91(17) Å$^3$ |
| Space group | P 21/a |
| Hall group | -P 2yab |
| Moiety formula | C37 H29 N2 O, Br [+ solvent] |
| Dx, g cm$^{-3}$ | 1.178 |
| Z | 4 |
| Mu (mm$^{-1}$) | 1.875 |
| F000 | 1232.0 |
| h, k, l max | 11,21,25 |
| Nref | 6383 |
| Tmin, Tmax | 0.894, 0.928 |
| Data completeness= 0.986 | Theta(max)= 69.890 |
| R(reflections)= 0.0656 (4273) | wR2(reflections)= 0.2194 (6295) |

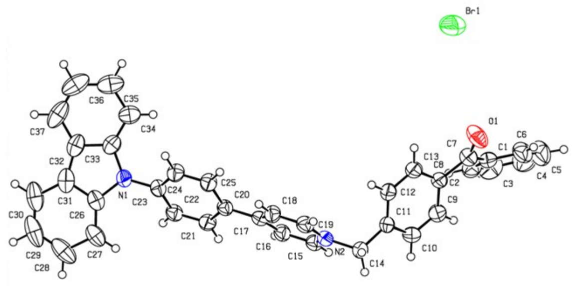


**Figure S40.** Single crystal X-ray structure of CZ-Pyr-BP.

**Table S3**. Crystal data and structure refinement for CZ-Pyr-BP.

| | |
|---|---|
| Empirical formula | $C_{37}H_{27}N_2OBr$ |
| Formula weight | 595.51 |
| Temperature | 294 K |
| Wavelength | 1.54184 |
| Bond precision | C-C = 0.0066 Å |
| Unit cell dimensions | a = 19.2347(8) Å alpha = 90 deg |
| | b = =8.0685(4) Å beta = 99.567(4) deg |
| | c = 20.4764(7) Å gamma = 90 deg |
| Volume | 3133.6(2) $Å^3$ |
| Space group | P 21/c |
| Hall group | -P 2ybc |
| Moiety formula | C37 H27 N2 O, Br [+ solvent] |
| Dx, g $cm^{-3}$ | 1.262 |
| Z | 4 |
| Mu ($mm^{-1}$) | 2.016 |
| F000 | 1224.0 |
| h, k, l max | 23,9,24 |
| Nref | 5929 |
| Tmin, Tmax | 0.841,0.902 |
| Data completeness= 0.984 | Theta(max)= 69.869 |
| R(reflections)= 0.0842 (4129) | wR2(reflections)= 0.2971 (5835) |

8. **The density functional theory (DFT) calculations of TPA-Pyr-Me, TPA-Pyr-BP, CZ-Pyr-Me and CZ-Pyr-BP.**

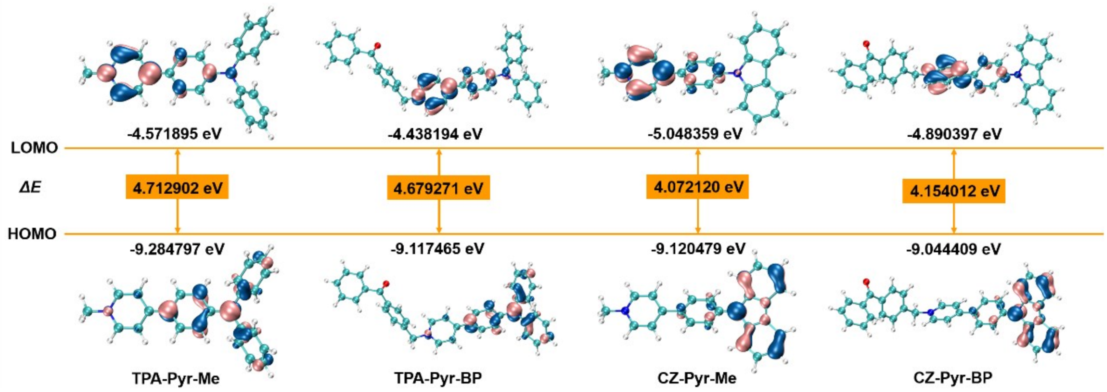


**Figure S41.** HOMO–LUMO energy levels of TPA-Pyr-Me, TPA-Pyr-BP, CZ-Pyr-Me and CZ-Pyr-BP, as estimated in Gaussian 16 using the CAM-B3LYP modification with the 6-311g(d) basis set.

9. **Fluorescence spectra at different temperatures of TPA-Pyr-BP.**

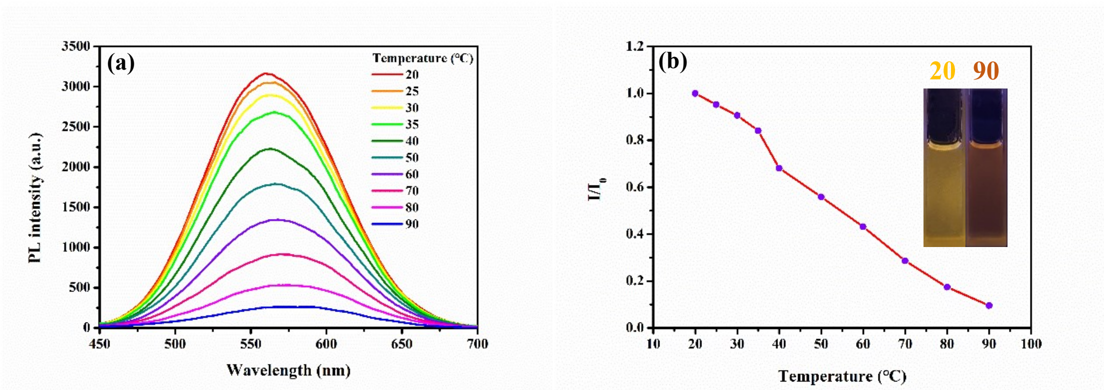


**Figure S42.** Change in the emission spectrum of TPA-Pyr-BP in glycerol and methanol mixture (95% glycerol) at different temperatures (concentration: 10 μM, $\lambda_{ex}$ = 430 nm). (B) The plot of the emission maximum of TPA-Pyr-BP at different temperatures. Inset shown the photographs of solution at 20 °C and 90 °C under illumination at 365 nm.

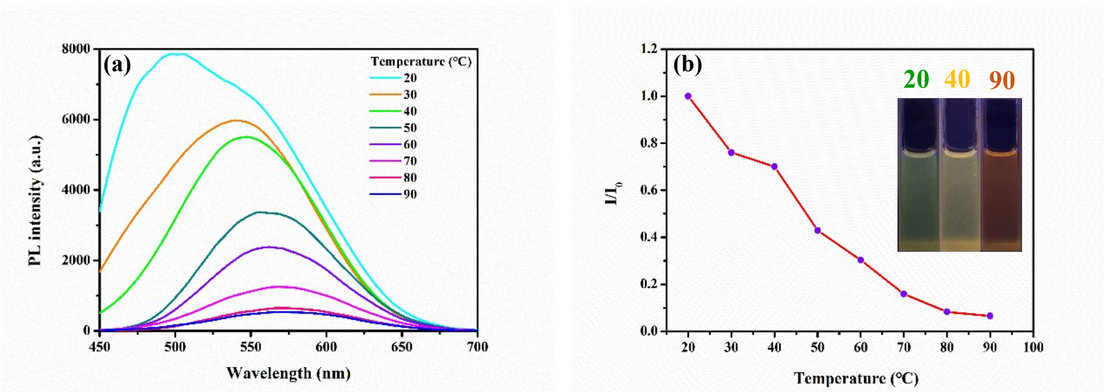


**Figure S43.** Change in the emission spectrum of TPA-Pyr-BP in glycerol and toluene mixture (95%

glycerol) at different temperatures (concentration: 10 μM, $\lambda_{ex}$ = 430 nm). (B) The plot of the emission maximum of TPA-Pyr-BP at different temperatures. Inset shown the photographs of solution at 20°C, 40 °C and 90 °C under illumination at 365 nm.

## 10. "ML" letter on the filter paper.


**Figure S44.** Images of TPA-Pyr-BP, TPA-Pyr-Me and CZ-Pyr-BP thin films on filter papers with letters of 'ML' being written by using a metal tweezers.

## 11. Umbrella patterns are painted on the filter paper.

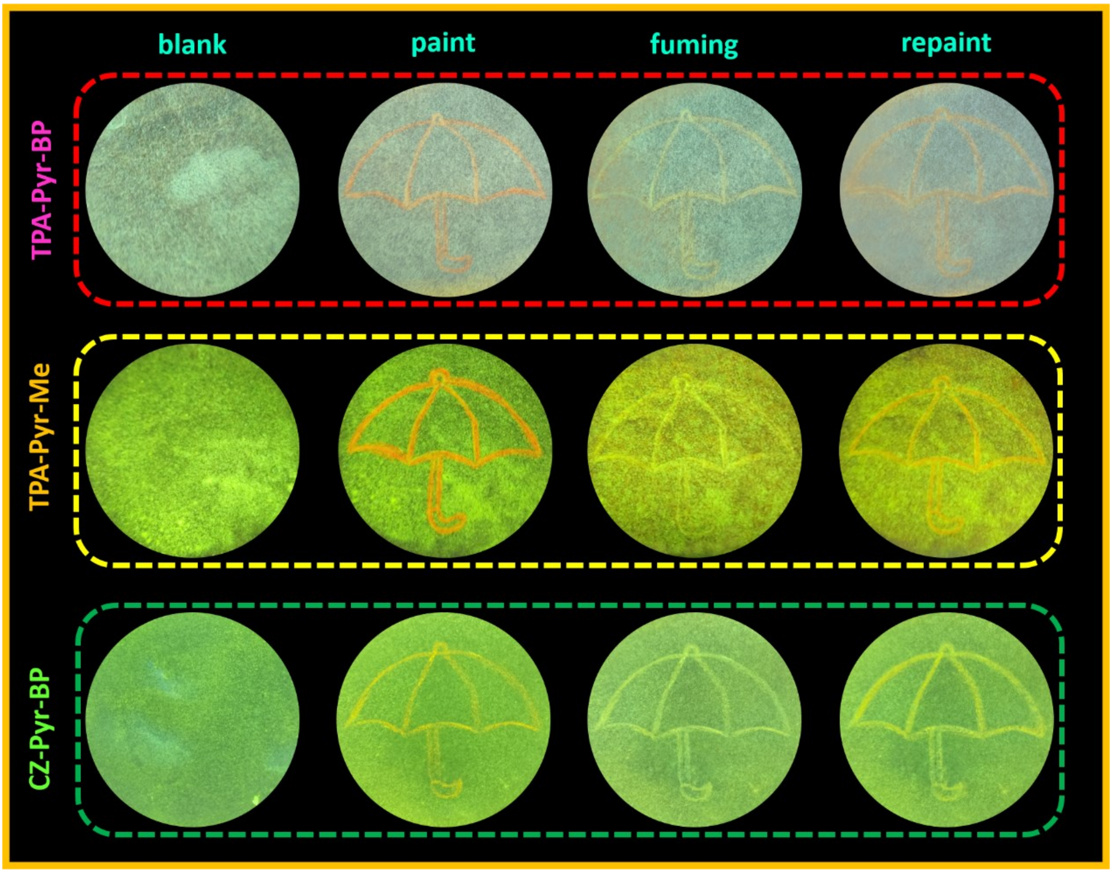


**Figure S45.** Images of TPA-Pyr-BP, TPA-Pyr-Me and CZ-Pyr-BP thin films on filter papers with graph of 'umbrella' being painted by using hollow ballpoint pen. The photos are blank control (filter paper wetted by the solution of TPA-Pyr-BP (in toluene) and then dried), umbrella patterns are painted by using hollow ballpoint pen on the filter paper, the fuming and repainted umbrella pattern, respectively.

Reference

1 K. M. Tan, Y. Zeng, L. Su, S. Q. Wang, X. D. Guo, Q. X Li, L. H. Xie, Y. Qian, Y. P. Yi, W. Huang, Molecular Dual-Rotators with Large Consecutive Emission Chromism for Visualized and High-Pressure Sensing, *ACS Omega*, 2018, **3**, 717-723.

2 J. Zhang, B. Z. He, W. J. Wu, P. Alam, H. Zhang, J. Y. Gong, F. Y. Song, Z. Y. Wang, H. M. H. Y. Sung, I. D. Williams, Z. M. Wang, J. W. Y. Lam, B. Z. Tang, Molecular Motions in AIEgen Crystals: Turning on Photoluminescence by Force-Induced Filament Sliding, *J. Am. Chem. Soc.,* 2020, **142**, 34, 14608-14618.

3 B. Wang, C. Y. Wei, Stimuli-responsive Flfluorescence Switching of Cyanostilbene Derivatives: Ultrasensitive Water, Acidochromism and Mechanochromism, *RSC Adv*., 2018, **8**, 22806-22812.

4 Y. X. Xu, K. Wang, Y. J. Zhang, Z. Q. Xie, B. Zou, Y. G. Ma, Fluorescence Mutation and Structural Evolution of a p-conjugated Molecular Crystal During Phase Transition, *J. M*ater. *Chem. C*, 2016, **4**, 1257-1262.

5 J. W. Sun, X. J. Lv, P. J. Wang, Y. J. Zhang, Y. Y. Dai, Q. C. Wu, M. Ouyang, C. Zhang, A Donor-acceptor Cruciform p-system: High Contrast Mechanochromic Properties and Multicolour Electrochromic Behavior, *J. Mater. Chem. C*, 2014, **2**, 5365-5371.

6 C. F. Feng, K. Wang, Y. X. Xu, L. Q. Liu, B. Zou, P. Lu, Unique Piezochromic Fluorescence Behavior of Organic Crystal of Carbazole-substituted CNDSB, *Chem. Commun***.**, 2016, **52**, 3836-3839.

7 H. S. Yuan, K. Wang, K. Yang, B. B. Liu, B. Zou, Luminescence Properties of Compressed Tetraphenylethene: The Role of Intermolecular Interactions, *J. Phys. Chem. Lett*., 2014, **5**, 2968-2973.